

University of Nebraska - Lincoln

DigitalCommons@University of Nebraska - Lincoln

Chemical & Biomolecular Engineering Theses,
Dissertations, & Student Research

Chemical and Biomolecular Engineering,
Department of

Spring 5-2015

Titanium Dioxide Nanoparticles Trigger Loss of Hepatic Function and Perturbation of Mitochondrial Dynamics in Primary Hepatocytes

Vaishaali Natarajan

University of Nebraska-Lincoln, vaishaali.n@gmail.com

Follow this and additional works at: <http://digitalcommons.unl.edu/chemengtheses>



Part of the [Chemical Engineering Commons](#)

Natarajan, Vaishaali, "Titanium Dioxide Nanoparticles Trigger Loss of Hepatic Function and Perturbation of Mitochondrial Dynamics in Primary Hepatocytes" (2015). *Chemical & Biomolecular Engineering Theses, Dissertations, & Student Research*. Paper 25.
<http://digitalcommons.unl.edu/chemengtheses/25>

This Article is brought to you for free and open access by the Chemical and Biomolecular Engineering, Department of at DigitalCommons@University of Nebraska - Lincoln. It has been accepted for inclusion in Chemical & Biomolecular Engineering Theses, Dissertations, & Student Research by an authorized administrator of DigitalCommons@University of Nebraska - Lincoln.

TITANIUM DIOXIDE NANOPARTICLES TRIGGER LOSS OF
HEPATIC FUNCTION AND PERTURBATION OF
MITOCHONDRIAL DYNAMICS IN PRIMARY
HEPATOCYTES

by

Vaishaali Natarajan

A THESIS

Presented to the Faculty of
The Graduate College at the University of Nebraska
In Partial Fulfillment of Requirements
For the Degree of Master of Science

Major: Chemical Engineering

Under the Supervision of Professor Srivatsan Kidambi

Lincoln, Nebraska

May 2015

TITANIUM DIOXIDE NANOPARTICLES TRIGGER LOSS OF HEPATIC
FUNCTION AND PERTURBATION OF MITOCHONDRIAL DYNAMICS IN
PRIMARY HEPATOCYTES

Vaishaali Natarajan, M.S.

University of Nebraska, 2015

Adviser: Srivatsan Kidambi

Titanium dioxide (TiO₂) nanoparticles are one of the most highly manufactured nanomaterials in the world with applications in copious industrial and consumer products. The liver is a major accumulation site for many nanoparticles, including TiO₂, directly through intentional ingestion or indirectly through increased environmental contamination and unintentional ingestion via water, food or animals. Growing concerns over the current usage of TiO₂ coupled with the lack of mechanistic understanding of its potential health risk is the motivation for this study. Here we determined the toxic effect of three different TiO₂ nanoparticles (commercially available rutile, anatase and P25) on primary rat hepatocytes. Specifically, we evaluated events related to hepatic functions and mitochondrial dynamics: (1) urea and albumin synthesis using colorimetric and ELISA assays, respectively; (2) redox signaling mechanisms by measuring ROS production; (3) OPA1 and Mfn-1 expression that mediates the mitochondria dynamics by PCR; and (4) mitochondrial morphology by MitoTracker Green FM staining. All three TiO₂ nanoparticles induced a significant loss in hepatic functions even at concentrations as low as 20 µg/ml with commercially used P25 causing maximum damage. TiO₂ nanoparticles

induced a strong oxidative stress in primary hepatocytes. TiO₂ nanoparticles exposure also resulted in morphological changes in mitochondria and significant loss in the fusion process, thus impairing the mitochondrial dynamics. Although this study demonstrated that TiO₂ nanoparticles exposure resulted in significant damage in primary hepatocytes, more *in vitro* and *in vivo* studies are required to determine the complete toxicological mechanism on primary hepatocytes and subsequently liver function.

ACKNOWLEDGEMENTS

I would like to thank the many people that made this work possible. I would like to thank my mentor Dr. Srivatsan Kidambi for inspiring me to try my best and for always being available for guidance and advice. I would like to thank my family, Amma, Appa and Varsha for being supportive and for being extremely understanding when I failed to keep in touch for long durations. I would like to thank my lab family Christina, Steve and Amita for all the wonderful discussions, research-related and otherwise, and for being the support system that never fails. I would also like to thank Dr. Edward Harris, Dr. Velandar and Dr. Saraf for their valuable inputs and perspectives that were necessary for shaping the project. I would like to thank all my friends in Lincoln that make Lincoln feel like home away from home. Last but not the least, I would like to thank Jagan for being there always, and for the unconditional support and positivity.

Table of Contents

LIST OF TABLES	iv
LIST OF FIGURES	v
List of Acronyms	vii
Chapter 1 Thesis Introduction and Background	1
1.1 Nanotechnology and Titanium Dioxide (TiO ₂) Nanoparticles:	1
1.2 Nanotoxicology:	2
1.3 Titanium Dioxide Nanoparticle Toxicity:	2
1.4 The liver and Nanoparticle toxicity:.....	5
Thesis Overview:	7
Chapter 2 Characterization of Titanium Dioxide Nanoparticles	8
2.1 Introduction	8
2.1.1 Importance of Nanoparticle Characterization:	8
2.1.2 Nanoparticle Selection for the Study:	9
2.2 Materials and Methods	10
2.2.1 Preparation of TiO ₂ nanoparticle suspensions	10
2.2.2 Dynamic Light Scattering	10
2.2.3 Transmission Electron Microscopy	10
2.3 Results	11
2.3.1 Aggregation and Surface Charge of the Nanoparticles.....	11
2.3.2 Particle Size and Shape of the Nanoparticles	11
2.4 Discussion	14
2.4 Conclusion.....	15
Chapter 3 Effect of Titanium Dioxide Nanoparticles on Primary Hepatocyte Viability and Functions.....	16
3.1 Introduction	16
3.1.1 TiO ₂ Nanoparticles mediated Toxicity to The Liver	16
3.1.2 Primary Hepatocytes as <i>in vitro</i> Liver Models	17
3.2 Materials and Methods	17
3.2.1 Isolation of Primary Hepatocytes.....	17
3.2.2 Culture and Treatment of Primary Hepatocytes	19

3.2.3 Cytotoxicity Assay to Determine LC ₅₀	19
3.2.4 Scanning Electron Microscopy (SEM).....	20
3.2.5 Live Dead Fluorescent Assay.....	20
3.2.6 Urea Quantification Assay.....	20
3.2.7 Albumin Quantification ELISA.....	21
3.2.8 Cell Morphology Analysis:.....	21
3.2.9 Statistical Analysis:.....	21
3.3 Results.....	22
3.3.1 Cytotoxicity of TiO ₂ Nanoparticles on Primary Hepatocytes.....	22
3.3.3 TiO ₂ Nanoparticles and Primary Hepatocyte Cell Viability.....	25
3.3.3 TiO ₂ Nanoparticles and Primary Hepatocyte Specific Functions.....	28
3.4 Discussion.....	33
3.4 Conclusion.....	37
Chapter 4 Mechanistic Aspects of Titanium Dioxide Mediated Toxicity.....	38
4.1 Introduction.....	38
4.1.1 Titanium Dioxide and Oxidative Stress.....	38
4.1.2 The Liver and Mitochondria.....	38
4.2 Materials and Methods.....	40
4.2.1 Reactive Oxygen Species (ROS) Quantification.....	40
4.2.2 Gene Expression Studies.....	41
4.2.3 Mitochondrial Morphology Imaging.....	42
4.2.4 Statistical Analysis.....	42
4.3 Results.....	43
4.3.1 Titanium Dioxide Nanoparticles and Oxidative Stress.....	43
4.3.2 Titanium Dioxide Nanoparticles and Mitochondrial Dynamics.....	44
4.3.2 Titanium Dioxide Nanoparticles and Mitochondrial Morphology.....	45
4.4 Discussion.....	47
4.5 Conclusion.....	49
Chapter 5 Conclusions.....	50
Chapter 6 Future Studies.....	52
Bibliography.....	53

LIST OF TABLES

Table 1. Characterization of TiO ₂ nanoparticles aggregates forming in hepatocyte culture medium using Dynamic Light Scattering (DLS) at 37 °C and pH of 7.4.	12
Table 2: Lethal Concentration (LC50) analysis of the different TiO ₂ nanoparticles treatment of primary rat hepatocytes.	22

LIST OF FIGURES

Figure 1. Quantification of Titanium Dioxide Nanoparticles in Various Cosmetic Products	3
Figure 2. Quantification of Titanium Dioxide Nanoparticles in Various Food Product Groups.....	4
Figure 3 Consumption of TiO ₂ according to age group.....	4
Figure 4. Schematic Representation of Rutile and Anatase Crystal shapes of Titanium Dioxide Nanoparticles	9
Figure 5. Comparison of Hydrodynamic Diameters of Nanoparticles in Different Concentrations	12
Figure 6. Transmission Electron Microscopy images to characterize the crystal shape of the TiO ₂ NPs as seen in DI water; (a) P25, (b) Anatase, 50 nm particle size and (c) Rutile , 50 nm particle size, scale = 50 nm.....	13
Figure 7. Dose response curve to calculate LC50 using four parameter plots for the different titanium dioxide nanoparticle treatment on primary hepatocytes.....	23
Figure 8. Scanning Electron Microscopy (SEM) images to visualize the morphology of primary hepatocytes when treated with TiO ₂ nanoparticles after 72 h of exposure. Scale bar: 30 microns. Yellow arrows point to primary hepatocytes.....	24
Figure 9. MTT assay to quantify primary hepatocyte viability after treatment with different TiO ₂ nanoparticles at 20, 50 and 100 µg/ml after 72 h of exposure normalized to the untreated hepatocytes. * p value < 0.001	26
Figure 10. Live/Dead dual fluorescent staining of primary hepatocytes when treated with titanium dioxide nanoparticles on Day 7 in culture. Calcein FM stains the live cells green and Ethidium Bromide stains the dead cells red. Scale bar: 100 microns.	27
Figure 11. Characterizing the effect of the different TiO ₂ nanoparticles treatment on primary hepatocytes specific functions; Quantification of urea synthesized primary hepatocytes after 72 h of exposure normalized to the untreated cells * p value < 0.001, 29	29
Figure 12. Quantification of urea synthesized primary hepatocytes from day 1 to day 7 in culture when treated with the different TiO ₂ nanoparticles. All the data points are normalized to untreated hepatocytes.....	30
Figure 13. Characterizing the effect of the different TiO ₂ nanoparticles treatment on primary hepatocytes specific functions; Quantification of albumin synthesized primary hepatocytes after 72 h of exposure normalized to the untreated cells * p value < 0.001, # p value 0.01	32
Figure 14. Quantification of albumin synthesized primary hepatocytes from day 1 to day 7 in culture when treated with the different TiO ₂ nanoparticles. All the data points are normalized to untreated hepatocytes.....	33
Figure 15. Characterizing the effect of nanoparticle treatment on primary hepatocyte mitochondrial functions; Quantification of Reactive Oxygen Species produced by primary	

hepatocytes using DCFDA based fluorescence assay after treatment with the different TiO ₂ nanoparticles for a duration of 72 h. Significant difference with respect to control is denoted as * p value < 0.0001, # p value < 0.05	43
Figure 16. Characterizing the effect of nanoparticle treatment on primary hepatocyte mitochondrial functions; Relative gene expressions of mitochondrial fusion markers when primary hepatocytes are treated with nanoparticles at a concentration of 50 µg/ml as analysed using qPCR with GAPDH as housekeeping gene. Significant difference with respect to control is denoted as * p value < 0.001 and # p value < 0.05	44
Figure 17. Fluorescent imaging of the mitochondrial morphology in primary rat hepatocytes after treatment with the different TiO ₂ nanoparticles at a concentration of 50ppm using Mitotracker green FM. Scale 20 microns.....	46
Figure 18. Schematic representation of the possible damaging role of TiO ₂ nanoparticles on primary hepatocytes. We propose that TiO ₂ induces loss in hepatic functions on primary hepatocytes through the induction of oxidative stress mediated by an increase of ROS production, and significant mitochondria damage by down-regulating the fusion cycle in the mitochondrial dynamics.....	51

List of Acronyms

ANOVA	Analysis of variance
DMEM	Dulbeccos's Modified Eagle's Medium
qPCR	Quantitative Polymerase Chain Reaction
PBS	Phosphate Buffer Saline
TiO ₂	Titanium Dioxide
cDNA	Complementary DNA
Opa1	Optical Atrophy 1
Mfn1/2	Mitofusins 1/2
EGF	Epidermal Growth Factor
IACUC	Institutional Animal Care and Use Committees

Chapter 1 Thesis Introduction and Background

1.1 Nanotechnology and Titanium Dioxide (TiO₂) Nanoparticles:

In the last two decades, Nanotechnology has revolutionized industries as diverse as engineering, health science and information technology.¹ Novel materials with valuable nanoscale properties are being discovered and engineered on large scale to meet with the increasing demands in the fields of application. Engineered nanoparticles form a major fraction of man-made nanomaterials that is increasing rapidly, escalating in both development and commercial implementation in applications such as drug delivery systems, antibacterial materials, cosmetics, biosensors, tissue engineering and electronics, yielding over thousands of consumer-based products already available in the market.²

Among engineered nanoparticles, titanium dioxide (TiO₂) ranks as one of the most highly manufactured and consumed type, from the perspective of both consumer products and research applications.^{2 3 4} These metal nanoparticles are commercially synthesized in rutile and anatase crystal forms. Nanoparticles of TiO₂ possess significantly different physicochemical properties, compared to the bulk phase, like strong catalytic activity, high refractive index, stability and photo sensitivity.² These unique properties render the TiO₂ nanoparticles very versatile and find them applications in a wide spectrum of industries ranging from water treatment, cosmetics, paint sunscreens, air cleaning, foods, sterilization, implants, to pharmaceuticals.^{4 5 6 7 8 9 10}

1.2 Nanotoxicology:

Despite the growing popularity, the largely different repertoire of physicochemical properties of nanomaterials gives rise to concerns over their bioactivity profile. Nanoparticles are exploited for properties such as small size, increases surface area, higher reactivity, aggregation potential, and different optical and electrical properties, as compared to their bulk phase counterparts. These differences influence the nature of interaction of nanomaterials with biological and ecological systems that were not a concern with the bulk material. For example, small particles can enter cells with ease and interact with the intracellular macromolecules.¹¹ They can escape conventional phagocytic responses and gain access to circulation and nervous system.¹ Inhalation of nano-dimensioned material can gain it easy access to respiratory system and the brain.² Apart from the inherent material properties, the synthesis technique, the route of exposure and level of exposure (acute, chronic or sub-chronic) understandably play a crucial role in their nature of interaction with biological systems.

In the event of these concerns, the US Environmental Protection Agency (EPA) and other central environmental bodies have expressed their concerns about potential toxicity of nanoparticles and are considering measures to limit the use in commercial products and increase the government regulations.¹²

1.3 Titanium Dioxide Nanoparticle Toxicity:

Metal nanoparticles such as Titanium Dioxide have been used in a variety of common consumer products such as food, cosmetics, air/water purifier, medicines, toothpastes and

sunscreens.³ Due to the abundance of commonly found products that contain TiO₂, there is a high chance of repeated exposure to these particles.

Various routes of exposure that can lead to the systemic availability of these nanoparticles and the most common ones are oral, subcutaneous, dermal, intravenous and lastly, respiratory. Respiratory exposure risks are particularly elevated in the form of occupational hazard. Previous reports show that over 150 different cosmetic products can lead to long term dermal exposure of titanium dioxide nanoparticles (**Fig. 1**). The whitening properties of TiO₂ nanoparticles renders them useful as a food colorant. A recent study demonstrates the various common food products that have these nanoparticles in them (**Fig. 2**), along with the likely daily exposure to humans of various age groups (**Fig. 3**).³ Repeated use of TiO₂ containing nanoparticles can lead to chronic level exposure and accumulation in various organs.

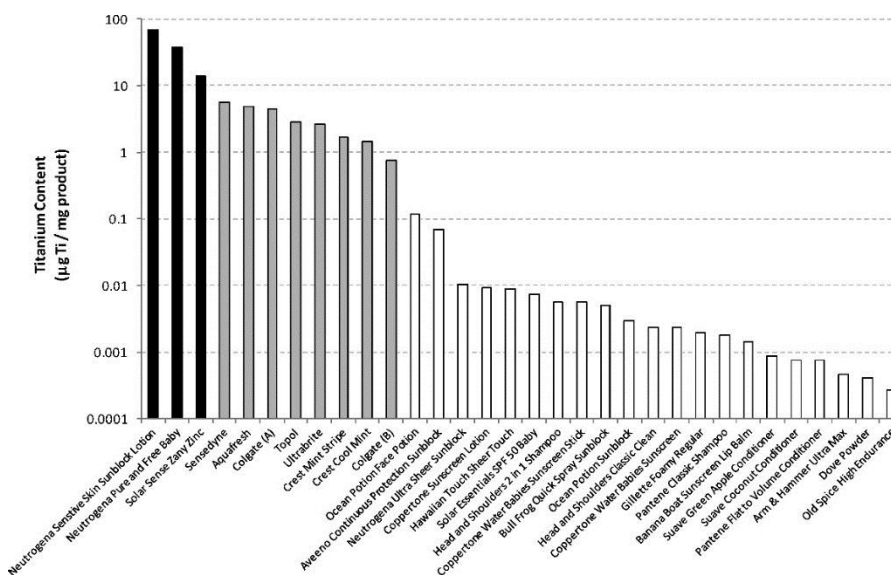


Figure 1. Quantification of Titanium Dioxide Nanoparticles in Various Cosmetic Products

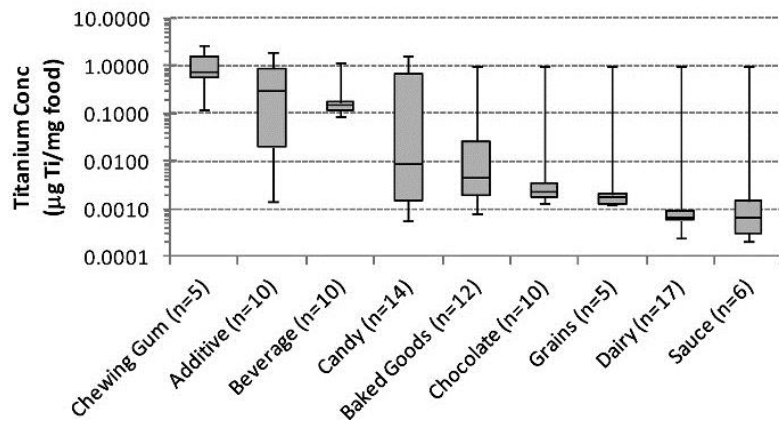


Figure 2. Quantification of Titanium Dioxide Nanoparticles in Various Food Product Groups

Published in: Alex Weir; Paul Westerhoff; Lars Fabricius; Kiril Hristovski; Natalie von Goetz; *Environ. Sci. Technol.* **2012**, 46, 2242-2250. Copyright © 2012 American Chemical Society

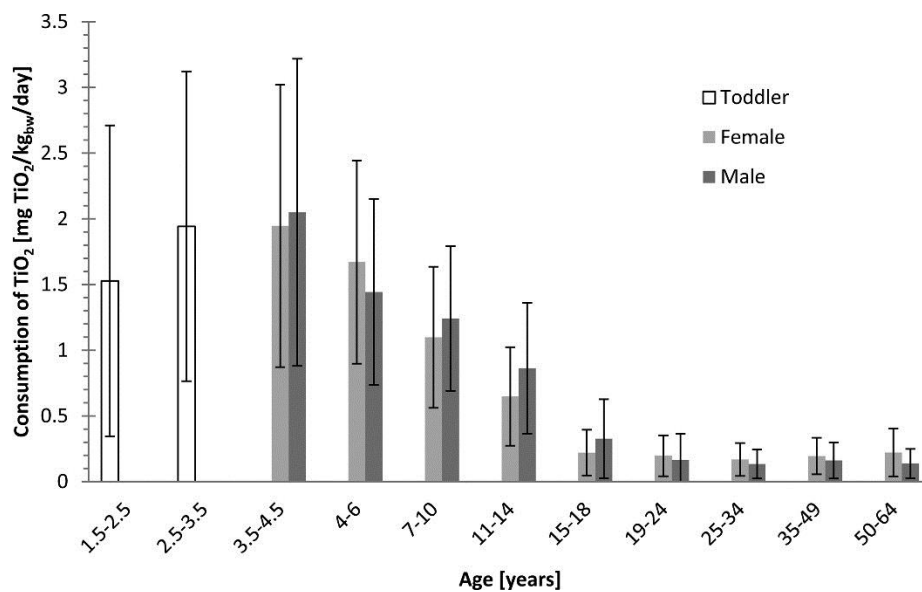


Figure 3 Consumption of TiO₂ according to age group

Published in: Alex Weir; Paul Westerhoff; Lars Fabricius; Kiril Hristovski; Natalie von Goetz; *Environ. Sci. Technol.* **2012**, 46, 2242-2250. Copyright © 2012 American Chemical Society

Several research groups have studied the toxicological behavior of TiO₂ nanoparticles using *in vivo* and *in vitro* models. The effects elicited by these particles on the respiratory system are most elaborately studied.^{13 14 15} Multiple studies on animal models have shown that exposure to TiO₂ nanoparticles has led to detrimental responses like Reactive Oxygen Species (ROS) generation, increased immune response, triggering of inflammation and accumulation in the system. Multiple cases of *in vitro* studies on various different sources of cells have also shown phenomena of apoptosis and genotoxicity, upon exposure of these nanoparticles.

1.4 The liver and Nanoparticle toxicity:

The liver is a multicellular organ that performs numerous vital metabolic, synthetic and clearance-related functions in mammals. Hepatocytes account for approximately 80% of the liver mass and perform essential metabolic functions in the normal and diseased liver. Studies demonstrate that the liver is a major accumulation site for many nanoparticles, directly through intentional ingestion or indirectly through nanoparticle dissolution from food containers or secondary ingestion of inhaled particles.^{11, 16-18} Additionally, increased environmental contamination and unintentional ingestion via water, food or animals may also result in further contact and subsequent accumulation of nanoparticles in the liver.^{11, 19, 20} Being the primary site for exposure to numerous nanoparticles renders the liver a high risk-site for damage from these foreign materials.

Studies on the bio-distribution of TiO₂ nanoparticles have depicted the liver as one of the principal sites in the body for accumulation.^{16, 21} The concern about adverse health effects of low-level exposure to TiO₂ is imperative to address, particularly study regarding TiO₂

exposure leading to liver degeneration by impairing mitochondrial bioenergetics. As a means to address these concerns and to establish the toxicological profile of TiO₂ nanoparticles, various groups have studied the effects elicited by these particles on different biological systems, both *in vitro* and *in vivo*.^{13, 22} Few studies provide evidence of impaired mitochondrial bioenergetics and apoptotic cell degeneration after low-level exposure to TiO₂.^{23, 24} There is a plethora of published literature on acute TiO₂ toxicity, however, the effect of TiO₂ exposure on the hepatocyte mitochondria and its implications on liver remain to be investigated.

Thesis Overview:

This thesis focuses on identifying and characterizing titanium dioxide nanoparticles that are commonly used in commercial applications and investigating the perturbations in liver behavior and mitochondrial characteristics caused by exposure to these TiO₂ nanoparticles, in order to broaden our understanding on the molecular mechanisms of liver dysfunction induced by these highly utilized nanoparticles. Chapter 2 describes the preparation of nanoparticles suspensions and characterization. Chapter 3 focuses on developing primary rat hepatocytes as our model liver system to investigate the concentration and type dependent toxic effects of TiO₂ nanoparticles on hepatic functions. Chapter 4 describes our findings about the mechanistic aspects that could trigger the changes observed in primary hepatocytes, upon treatment with TiO₂ nanoparticles. Chapter 5 contains the overall summary of the results obtained and potential future directions that will aid in the deeper understanding of the effects of TiO₂ nanoparticles on the liver cells.

Chapter 2 Characterization of Titanium Dioxide Nanoparticles

2.1 Introduction

2.1.1 Importance of Nanoparticle Characterization:

Nanoparticle characterization plays an important role in interpreting and comparing the toxicological effects elicited by the different types of TiO₂ on the specific biological system. TiO₂ nanoparticles are typically available in the anatase or rutile crystal forms. Parameters such as particle size, crystal phase and aggregation potential influence their bio-activity.²⁵ Different crystal forms of the nanoparticle have previously been shown to elicit different toxicological responses. Anatase crystal has been shown to possess higher reactivity of the two crystal forms.²⁶ The mechanism of toxicity elicited by the particles are also different. Previous studies show that anatase crystals can lead to cell necrosis and membrane leakage. Some studies also show that generation of Reactive Oxygen Species (ROS) occurs, whereas a few groups observe otherwise.^{27 28} On the contrary, rutile particles were shown to initiate apoptosis through ROS formation.²⁸ Variations with respect to initial particle size have also been observed by several groups.²⁶ These different results demonstrate the importance of characterizing the physicochemical parameters of the nanoparticle type in question, in order to fully understand and profile the toxicological behavior elicited by it. **Fig. 4** is a cartoon representation of rutile and anatase crystal forms of TiO₂ nanoparticles.

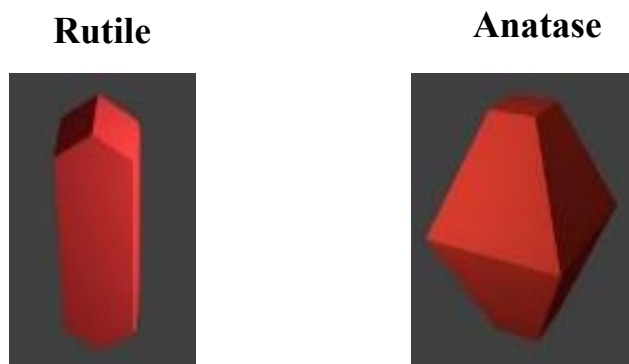


Figure 4. Schematic Representation of Rutile and Anatase Crystal shapes of Titanium Dioxide Nanoparticles

2.1.2 Nanoparticle Selection for the Study:

We chose three commercially available forms of TiO_2 nanoparticles (anatase, rutile and Degussa P25) for our study to determine their toxicological effects on primary rat hepatocytes. These particles were selected due to their higher potential of human exposure through abundance in consumer products and availability in water sources. Our study focused on investigating the crystal phase dependent effects of titanium dioxide nanoparticles on the cells. To keep crystal phase as the only variable, we chose pure rutile and pure anatase samples of same particle size of 50 nm. Degussa P25, a commercially available TiO_2 nanoparticle type is a mixture of both anatase and rutile. These three TiO_2 nanoparticles are referred to as anatase, rutile and P25 in the thesis hereon.

2.2 Materials and Methods

2.2.1 Preparation of TiO₂ nanoparticle suspensions

Degussa P25 was obtained from Sigma Aldrich, St. Louis, MO. Pure rutile 50nm, and pure anatase 50nm were purchased from MK Nano, Mississauga, Ontario, Canada. The nanoparticles were UV sterilized and stock suspensions were made in sterile Phosphate Buffer Saline (PBS) at pH 7.4, mixed for 2 minutes, sonicated [FS30D Fisher Scientific] for 30 min and stored in dark at 4 °C until use.

2.2.2 Dynamic Light Scattering

TiO₂ Nanoparticle size and zeta potential were measured using a NanoBrook ZetaPALS zeta potential and dynamic light scattering instrument [Brookhaven instrument, Holtsville, NY]. Desired concentrations of nanoparticle suspensions were prepared by dilution with Hepatocyte culture medium (described in Chapter 3). Mean hydrodynamic diameter was measured at a scattering angle of 90°, and the Zeta potential was calculated from Mobility measurements by using the Smoluchowski model. All measurements were performed at 25 °C at a pH of 7.4.

2.2.3 Transmission Electron Microscopy

Stable suspensions of the different nanoparticles was prepared in DI water using sonication. The samples were prepared for imaging by sequential drying steps on copper grids [Ted Pella, Inc., CA] that were coated with carbon. Hitachi H7500 TEM was used for analyzing the samples.

2.3 Results

2.3.1 Aggregation and Surface Charge of the Nanoparticles

TiO₂ nanoparticles aggregates in aqueous hepatocyte media were characterized using DLS. The purity of the starting nanoparticles was over 95%. To measure the hydrodynamic diameter of the aggregates and their resultant zeta potential, working concentration of nanoparticles suspension were prepared in hepatocyte media in the identical manner in which they are prepared for the cell culture studies. As shown in **Table. 1**, P25, anatase, and rutile nanoparticles aggregated to average diameter of approximately 800nm, 700nm, and 380nm, respectively. The aggregate hydrodynamic diameter did not vary significantly with the varying concentration of the nanoparticles, in all three sample types (**Fig. 5**). Zeta potential were also measured for the three TiO₂ nanoparticles (**Table. 1**). The zeta potential values did not change significantly in the three forms of the nanoparticles and in all three concentrations.

2.3.2 Particle Size and Shape of the Nanoparticles

TEM was used to define the individual crystal shapes and sizes of the different TiO₂ nanoparticles (**Fig. 6**). Anatase TiO₂ nanoparticles displayed the characteristic spherical crystal structure, with each particle size around 50nm and rutile nanoparticles displayed a typical rod-like crystal structure. P25, which is a 3:1 mixture of anatase and rutile, had crystals characteristic of both anatase and rutile. These results were in agreement with the manufacturer's specifications and previous reports on the characterization of the shape of the nanoparticles.^{21, 25, 26}

TiO ₂ Nanoparticle	Concentration	Hydrodynamic Diameter (nm)	Polydispersity Index	Zeta Potential (mV)
P 25	100 ppm	784.1 ± 54.5	0.226	-10.8 ± 2.5
	50 ppm	783.5 ± 57.4	0.157	-8.7 ± 3.5
	20 ppm	841.7 ± 85.3	0.279	-6.4 ± 2.4
Anatase	100 ppm	692.4 ± 59.4	0.178	-9.9 ± 4.3
	50 ppm	659.2 ± 35.0	0.166	-7.4 ± 2.8
	20 ppm	739.1 ± 86.9	0.232	-8.7 ± 4.3
Rutile	100 ppm	396.3 ± 13.5	0.248	-6.5 ± 4.3
	50 ppm	374.8 ± 34.5	0.189	-8.5 ± 4.6
	20 ppm	380.0 ± 29.1	0.236	-10.2 ± 1.8

Table 1. Characterization of TiO₂ nanoparticles aggregates forming in hepatocyte culture medium using Dynamic Light Scattering (DLS) at 37 °C and pH of 7.4.

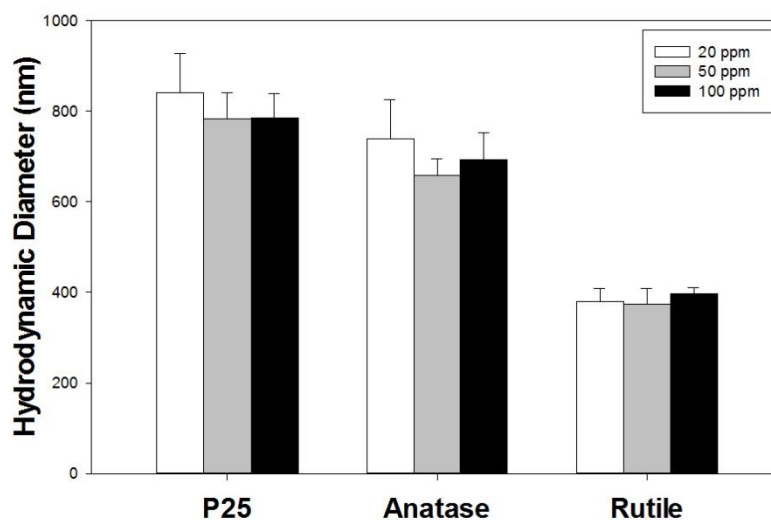


Figure 5. Comparison of Hydrodynamic Diameters of Nanoparticles in Different Concentrations

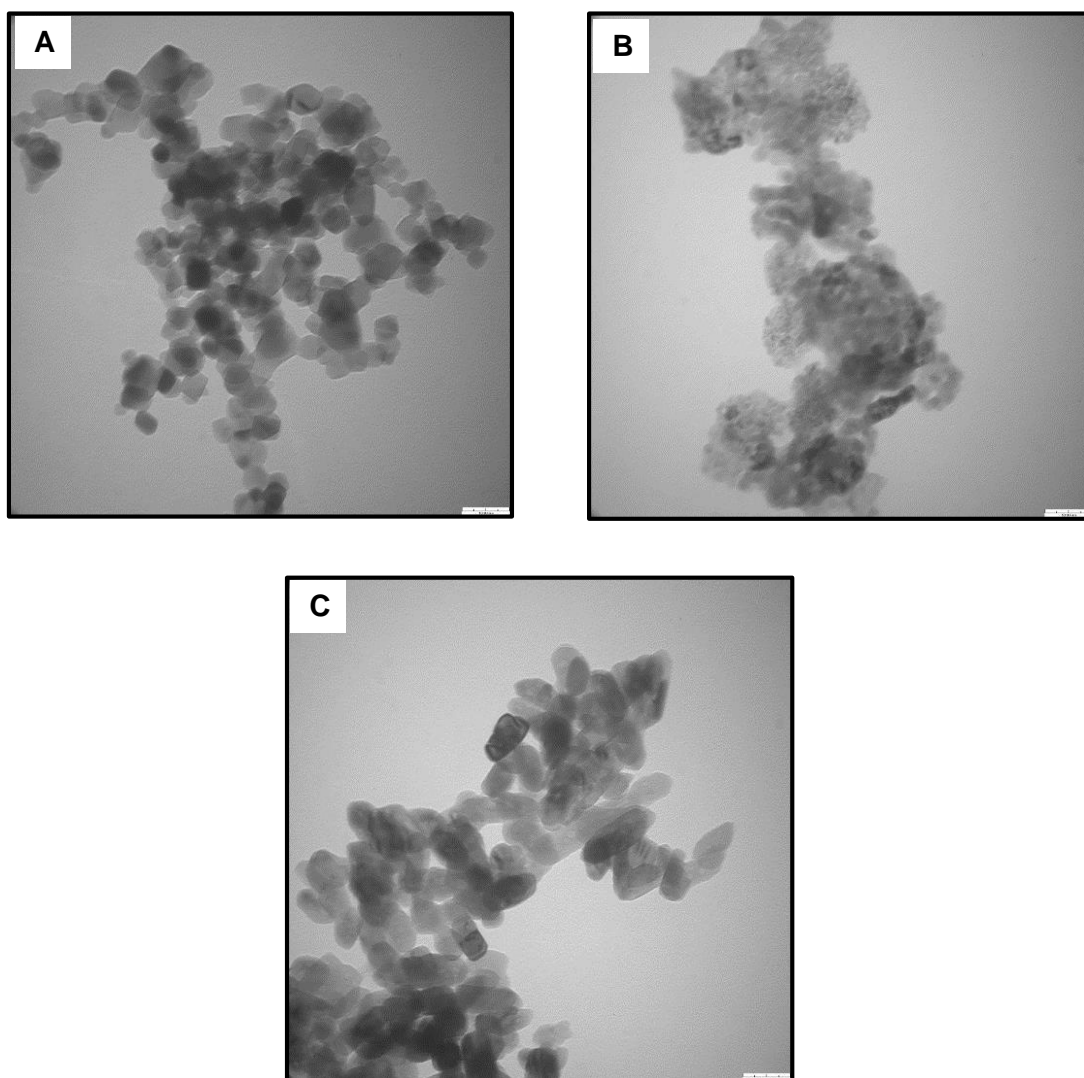


Figure 6. Transmission Electron Microscopy images to characterize the crystal shape of the TiO₂ NPs as seen in DI water; (a) P25, (b) Anatase, 50 nm particle size and (c) Rutile, 50 nm particle size, scale = 50 nm

2.4 Discussion

Nanoparticle characterization plays a vital role in interpreting and comparing the toxicological effects elicited by the different types of TiO₂ on the specific biological system. We chose three commercially available forms of TiO₂ nanoparticles (anatase, rutile and P25) for our study to determine their toxicological effects on primary rat hepatocytes. Our TEM results indicate that the crystal structure of anatase was spherical, rutile was rod shaped and P25 had a mixture of both the crystal structures. **(Fig. 6)** TiO₂ nanoparticles have the tendency to form aggregates in aqueous media that have high ionic strength. To compare the level of aggregation of the TiO₂ nanoparticles in physiologically relevant conditions including the presence of proteins and divalent ions, we studied the aggregation nature of the TiO₂ nanoparticles in serum containing hepatocyte culture media. As seen in **Table. 1**, the aggregation did not vary significantly with the concentration of the nanoparticle suspension, within the same type. For the variation of the aggregate sizes between the different nanoparticles, the type of crystal structure of the particles (anatase vs rutile) and the relative composition of the three forms of nanoparticles might attribute to the observed variations in their aggregation sizes.

In agreement with the aggregation in the physiologically relevant media, the zeta potential for all three TiO₂ crystalline forms, regardless of concentration, was measured to be within the realm of colloidal instability. Our extensive characterization provides us with valuable information about the physicochemical properties of the different type of particles the cells are interacting with when they are exposed to TiO₂.

2.4 Conclusion

We were able to characterize the individual particle shape and size using TEM and observed a typical crystal shape of rod-like in rutile and spherical in anatase, consistent with the previous reports on similar characterization. With the DLS study, we were able to characterize the hydrodynamic diameter and zeta potential of the different titanium dioxide nanoparticles in hepatocyte medium. These characterizations will prove useful in correlating our observations with the inherent physicochemical behavior of the particles.

Chapter 3 Effect of Titanium Dioxide Nanoparticles on Primary Hepatocyte Viability and Functions

3.1 Introduction

3.1.1 TiO₂ Nanoparticles mediated Toxicity to The Liver

Exposure routes such as respiratory, oral, intravenous and dermal have scope for systemic access to foreign particles. Previous reports on the bio-distribution of TiO₂ nanoparticles suggest high likelihood for the particles to reach the liver and accumulate.²²⁻²⁹ Study by Fabian et al demonstrates that traces of nanoparticles were found in the liver 28 days after intravenous exposure to anatase and rutile TiO₂ nanoparticles.³⁰ Cui et al showed that prolonged intra-gastric instillation of TiO₂ Nanoparticles causes NF κB mediated inflammation, followed by apoptosis in the liver of mice models.³¹

Some recent in vitro studies have also investigated the toxicity of these metal nanoparticles on the liver cells. Shi et al showed that human L02 hepatocytes displayed increased oxidative stress due to ultrafine TiO₂ nanoparticle exposure.³² Similar results of oxidative stress were observed in BRL 3A rat liver cell line.³³

Limited number of studies have been carried out in order to explore the mechanistic aspects of TiO₂ Nanoparticles on hepatocytes. Studies carried out on animal models have the limitation of being complex and it is challenging to deduce the observations to a particular cell type without accounting for the exogenous factors. Similarly, use of hepatic cell lines pose the disadvantage of potential deviation from the actual liver biology owing to the transformations cell lines undergo.

3.1.2 Primary Hepatocytes as *in vitro* Liver Models

Hepatocytes are the most important cell type of the liver and perform numerous vital metabolic, storage and clearance related functions.³⁴ Primary hepatocytes retain a considerable fraction of their complex functions when cultured in suitable conditions *in vitro*. Prolonged culture of hepatocytes leads to loss in the differentiated phenotype and this event precedes cell death. To understand the cytotoxicity of nanoparticles, along with general end point assays such as quantification of viability and morphology, studying the hepatocyte specific phenotypic markers is essential. Hepatocyte specific functions like synthesis of albumin and urea are gold standard markers for characterizing the phenotypic stability of the cells.³⁴ We investigated how these functions were affected by the exposure. To be able to study cellular events prior to cell death, as a preliminary step before studying the cellular markers, we determined the cytotoxicity of the different types of TiO₂ Nanoparticles on primary hepatocytes in order to obtain the lethal concentration value (LC₅₀).

3.2 Materials and Methods

3.2.1 Isolation of Primary Hepatocytes

All animal procedures were carried out in accordance with the guidelines from IACUC of University of Nebraska-Lincoln. Excision of the liver followed by isolation of hepatocytes was performed as per the protocol of P.O Seglen and R.Blomhoff³⁵ with slight modifications. Sprague Dawley rats weighing about 160-200g were subjected to anesthetic-conditions in a desiccator chamber saturated with 30% isoflurane solution. The rats were kept in the chamber till the full effect of anesthesia was confirmed, which is

limpness of the body and deep respiration. The animal was moved to the surgery table and a syringe tube with isoflurane was secured on the snout for assuring prolonged unconsciousness. With bandage scissors and forceps, the entire abdominal cavity was exposed and vena porta was located. A strand of surgical thread was drawn beneath the vena port and an overhand knot was tied. Vein was cannulated with Insyte Autoguard catheter (18GA, 1.3x300mm, BD Biosciences). The needle was retracted and oxygenated Tris Buffer Saline (TBS) was supplied through the catheter at a flow rate of about 20mL/min and was continued till the liver turned loam colored. Liver was excised out of the abdominal cavity by cutting around all the tissues that attach it to the body. Liver was placed on a sieved funnel and buffer was allowed to continually flush the blood away. Digestion of the liver by collagenase digestion followed next. Collagenase solution of strength about 10 mg per 100 grams of rat's weight was prepared in 60 mL of Calcium containing buffer. The TBS flushing was brought to an end and collagenase was pumped in through a closed circuit. After about 15 minutes, the liver was transferred to a sterile dish containing buffer 1 and Glisson's capsule and extra tissues, if any, were peeled away. The liver was shook in the buffer to detach all the hepatocytes in the liver matrix. And the buffer loaded with cells was filtered through 100 μm followed by 30 μm to get a purer population of hepatocytes. The filtrate was centrifuged with buffer 3 and 150xg for 3 minutes and the process was repeated till the supernatant was clear and the pellet intact. The viability of hepatocytes was determined using trypan blue exclusion method, was also confirmed using percoll gradient. Viability of 85% and above was considered threshold for continuing with culture.

3.2.2 Culture and Treatment of Primary Hepatocytes

Before seeding, tissue culture plate surfaces were coated with 100 μ g/ml rat tail collagen type I solution prepared in 0.02 N acetic acid for 1 hour at 37 °C, washed and stored at 4 °C till use. Cells were seeded at a density of 100,000/cm² on the collagen coated plates. Nanoparticle suspensions in the desired concentrations were prepared in the culture media and added to the cells.

Hepatocyte Culture Medium: Culture media was made with high glucose DMEM supplemented with 10% FBS, 0.5 U/ml insulin, 20 ng/ml epidermal growth factor (EGF), 7 ng/ml glucagon, 7.5 mg/ml hydrocortisone, and 1% penicillin-streptomycin. All the reagents were obtained from Sigma-Aldrich.

3.2.3 Cytotoxicity Assay to Determine LC₅₀

The cytotoxicity of nanoparticles was assessed by MTT assay [3-(4,5-dimethylthiazol-2-yl)-2,5 diphenyl Tetrazolium Bromide] [Life Technologies, NY] which quantitatively evaluates the mitochondrial conversion of the MTT salt into purple formazan crystals.. Nanoparticle solution was removed and 0.5 mg/ml MTT working solution in DMEM was incubated on live cells at 37 °C for 2.5 hours. After incubation the working solution was removed and lysis buffer (0.1 N HCl in Isopropanol) added. The lysis buffer was transferred to a 96 well plate and absorbance values collected in an AD340 plate reader [Beckman Coulter, Brea, CA] at corrected 570/620 nm. Relative absorbance was used as the indicator for cell viability. Concentration range of 0 μ g/ml to 1000 μ g/ml for each nanoparticle was used to generate the dose response curve. SigmaPlot software was used to calculate LC₅₀ value for each type of nanoparticle.

3.2.4 Scanning Electron Microscopy (SEM)

Nanoparticle size and shape were assessed and viewed under a scanning electron microscope (SEM) [S-3000N, Hitachi Tokyo, Japan]. Cellular morphology and nanoparticle distribution was visualized by SEM. The cells were rinsed with PBS and fixed with 4% paraformaldehyde/PBS solution for 15 min. The paraformaldehyde solution was removed, samples rinsed with PBS and dehydrated with ethanol solutions (from 20 to 100%). The sample was incubated for 15 min at room temperature in each solution. The 100% ethanol solution was removed with hexamethyl disilazane [Sigma Aldrich, USA] and the sample was allowed to air-dry. The samples were then coated with gold-palladium (Au-Pd) and analyzed under the SEM.

3.2.5 Live Dead Fluorescent Assay

Cell viability was assessed using a Live/Dead Viability/Cytotoxicity Kit [L-3224 Invitrogen, Grand Island, NY]. In short, Nanoparticle supernatant was removed and cells were washed once with PBS and incubated at 37 °C for 30 min with assay reagent (4 μ M EthD-1 and 2 μ M Calcein in PBS) at 37 °C. The cells were removed and washed 3 times with PBS and viewed with an Axiovert 40 CFL [Zeiss, Germany] and X-Cite 120Q [Lumin Dynamics, Mississauga, Ontario, Canada].

3.2.6 Urea Quantification Assay

Urea secretion by hepatocytes in culture medium was assessed every 24 hours using Stanbio Urea Nitrogen (BUN) kit [Stanbio, Boerne, TX] using manufacturer's protocol. Briefly, the kit exploits the reaction between urea and diacetyl monoxime which results in

a color change with an absorbance of 520 nm read on AD 340 plate spectrophotometer [Beckman Coulter, Brea, CA].

3.2.7 Albumin Quantification ELISA

Albumin Secretion by hepatocytes into culture medium was measured every 24 hours using Rat Albumin ELISA Quantitation Kit from Bethyl Laboratories, Inc [Montgomery, TX] according to manufacturer's instructions. In short, a 96 well plate was coated with a coating antibody for 1 hour and blocked with BSA for 30 min. Standard/Sample was added to each well and incubated for 1 hour. HRP detection antibody was incubated for 1 hour followed by the addition of TMB Substrate solution which was developed in the dark for 15 min and absorbance read on AD340 plate spectrophotometer [Beckman Coulter, Brea, CA] at 450 nm.

3.2.8 Cell Morphology Analysis:

Phase contrast images of primary hepatocytes cultured on the different substrates were captured using an Inverted Microscope [Axiovert 40 CFL, Zeiss, Germany]. For fluorescent viewing of the cell morphology, Calcein AM staining was used [Life Technology, NY].

3.2.9 Statistical Analysis:

The difference between the various experimental groups was analyzed by a one-way analysis of variance (ANOVA) using the statistical analysis feature embedded in SigmaPlot Software using Tukey test. Q tests were employed to identify outliers in the data subsets. For statistical analysis of all data, $p < 0.05$ was used as the threshold for significance.

3.3 Results

3.3.1 Cytotoxicity of TiO₂ Nanoparticles on Primary Hepatocytes

We evaluated the cytotoxicity of three different TiO₂ nanoparticles (P25, anatase and rutile) that were selected due to their abundance in commercial products using MTT assay. A 72 h exposure to the three different TiO₂ nanoparticles of varying concentration (0-1000 µg/ml) to primary hepatocytes established the LC₅₀ value of the different particles. As seen in **Table. 2**, the LC₅₀ values of P25, anatase and rutile TiO₂ nanoparticles were 74.13±9.72 µg/ml, 58.35±4.76 µg/ml, and 106.81±11.24 µg/ml, respectively. **Fig. 7** represents the dose response curves plotted using Sigma Plot for the different nanoparticles using non-linear regression that were used to analyze the LC₅₀ values. After determining the LC₅₀ values, the concentrations of 20, 50 and 100 µg/ml were chosen for the rest of the studies to enable studying the cellular phenomena at a sub-acute dosage range.

Nanoparticle Type	LC₅₀ value (in µg/ml)
P 25	74.13 ± 9.72
Anatase	58.35 ± 4.76
Rutile	106.81 ± 11.24

Table 2: Lethal Concentration (LC50) analysis of the different TiO₂ nanoparticles treatment of primary rat hepatocytes.

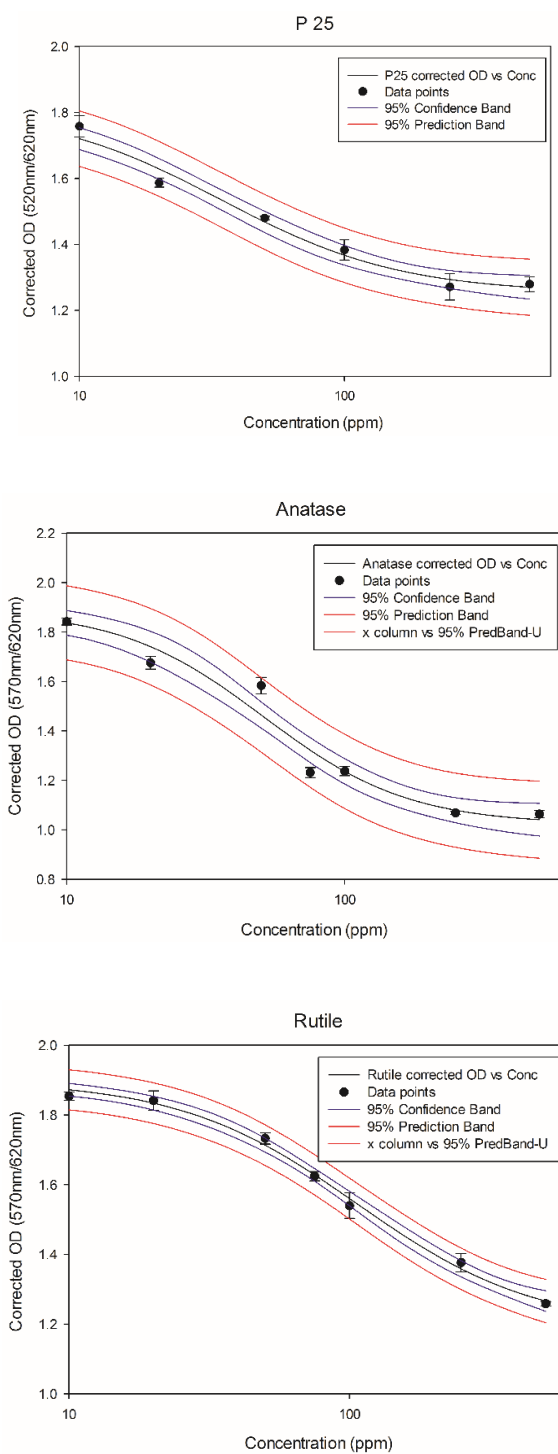


Figure 7. Dose response curve to calculate LC50 using four parameter plots for the different titanium dioxide nanoparticle treatment on primary hepatocytes

To study the concentration dependent effect of TiO₂ nanoparticles on primary hepatocyte morphology, we observed the cellular characteristics using SEM (**Fig. 8**). After 72 h of exposure to the three chosen concentrations of the nanoparticles, primary hepatocytes did not exhibit a marked change in cellular morphology. For all three nanoparticles we observed the smooth and spherical morphology of hepatocytes that was comparable to untreated cells.

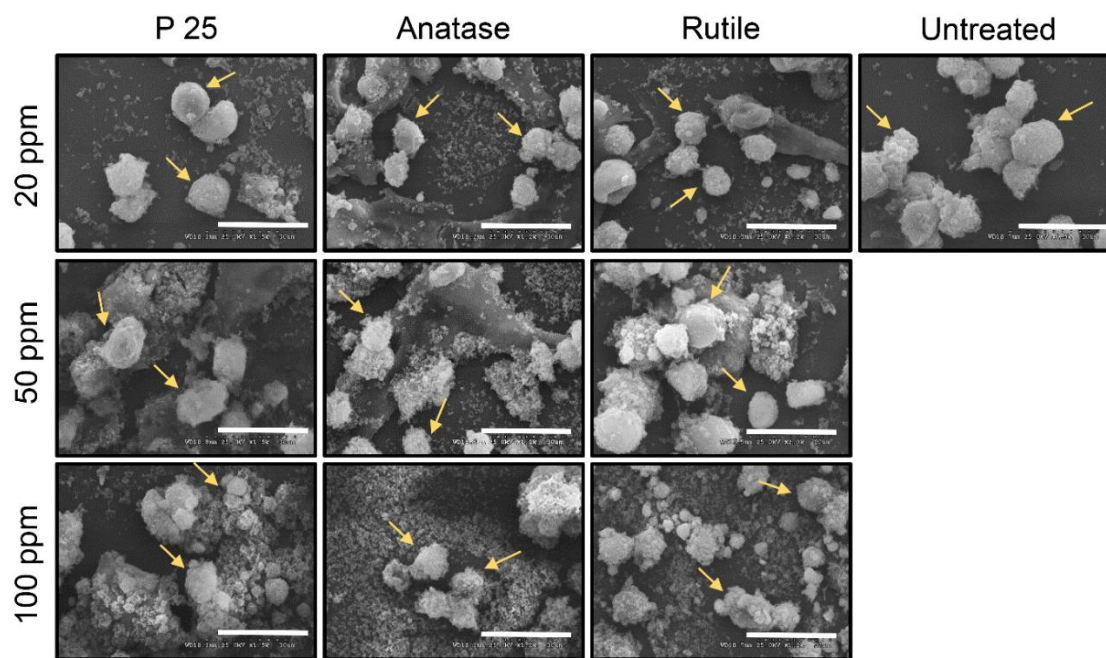


Figure 8. Scanning Electron Microscopy (SEM) images to visualize the morphology of primary hepatocytes when treated with TiO₂ nanoparticles after 72 h of exposure. Scale bar: 30 microns. Yellow arrows point to primary hepatocytes

3.3.3 TiO₂ Nanoparticles and Primary Hepatocyte Cell Viability

To quantitatively determine the viability loss in hepatocytes after exposure to TiO₂ nanoparticles, we performed MTT assay. Hepatocytes were treated in the chosen concentrations (20, 50 and 100 µg/ml) of P25, anatase, and rutile for 72 h. The exposure of hepatocytes to TiO₂ nanoparticles showed a concentration and type dependent loss in viability (**Fig. 9**). We normalized the viability of TiO₂ nanoparticles treated hepatocytes with respect to untreated cells. In P25 treated samples, 91% cells were viable when exposed to 20 µg/ml concentration which decreased to 75% at 100 µg/ml concentration. Similarly in hepatocytes exposed to anatase nanoparticles, the cell viability significantly decreased from 92% in the 20 µg/ml concentration to 66% in 100 µg/ml. However, all three concentrations of rutile did not affect the cell viability and had the highest percentage of viable cells even at a concentration of 100 µg/ml.

In addition, to study the effect of nanoparticle treatment after a prolonged duration, we performed Live/Dead Fluorescent cell staining as seen in **Fig. 10**. These results also suggest similar phenomenon. Anatase and P25 showed a greater loss in viability as compared to rutile and the effect was observed to be concentration dependent.

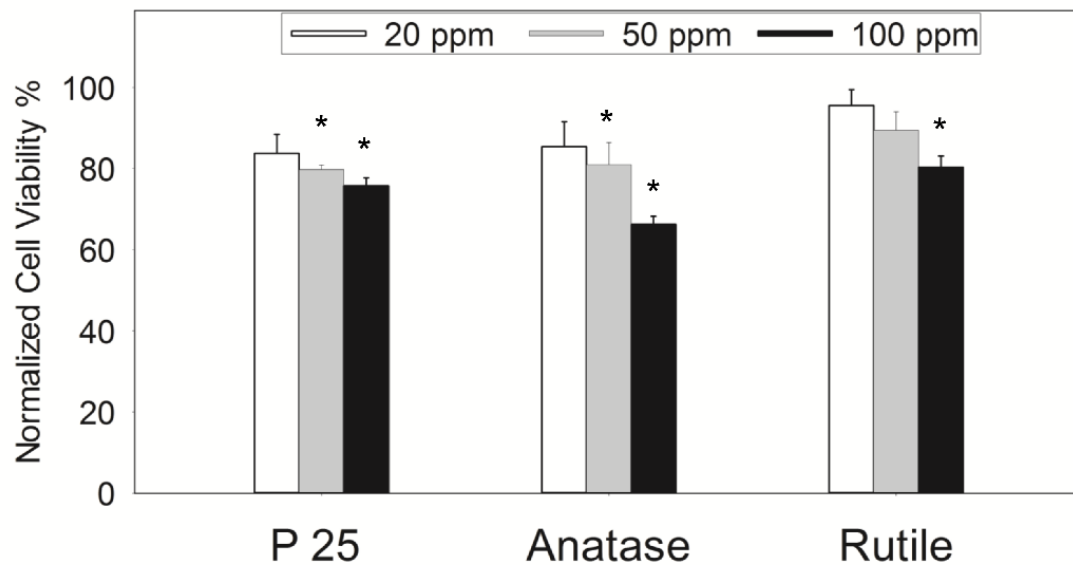


Figure 9. MTT assay to quantify primary hepatocyte viability after treatment with different TiO₂ nanoparticles at 20, 50 and 100 $\mu\text{g/ml}$ after 72 h of exposure normalized to the untreated hepatocytes. * p value < 0.001

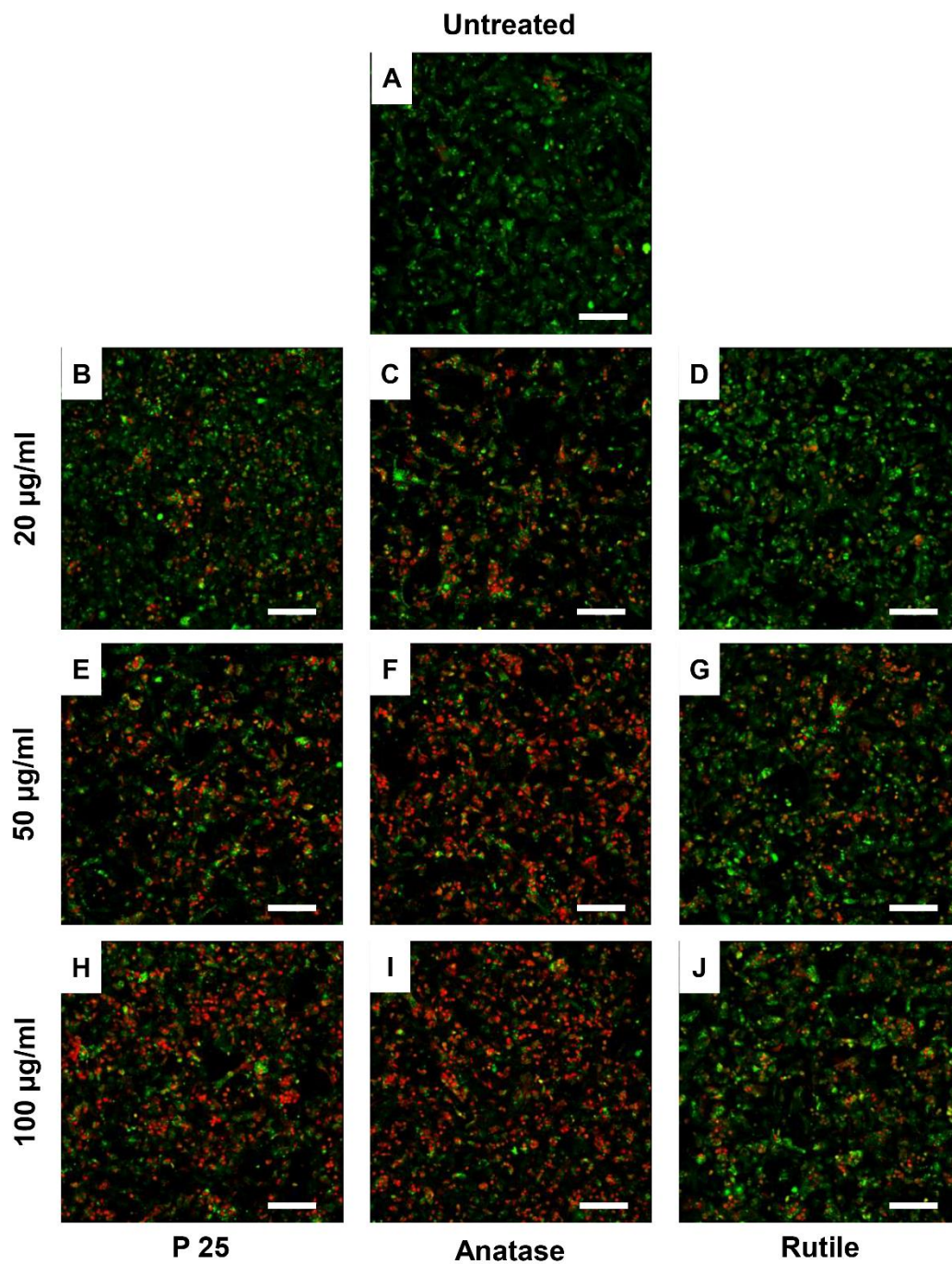


Figure 10. Live/Dead dual fluorescent staining of primary hepatocytes when treated with titanium dioxide nanoparticles on Day 7 in culture. Calcein FM stains the live cells green and Ethidium Bromide stains the dead cells red. Scale bar: 100 microns.

3.3.3 TiO₂ Nanoparticles and Primary Hepatocyte Specific Functions

3.3.3.1 Urea Synthesis

We studied the effect of prolonged exposure of hepatocytes to three chosen concentrations (20 µg/ml, 50 µg/ml, 100 µg/ml) and types of TiO₂ nanoparticles (P25, anatase, rutile) on two chief hepatic functions; urea synthesis and albumin synthesis. We quantified the amount of urea synthesized by hepatocytes upon treatment with TiO₂ nanoparticles, using a colorimetric assay (**Fig. 11** and **Fig. 12**). **Fig.11** illustrates the urea production of primary hepatocytes after 72 h of exposure to different TiO₂ nanoparticles. We normalized the value of urea and albumin synthesis of the treatment groups with respect to the untreated cells. We observed significant concentration and type dependent loss in urea synthesis. The exposure of hepatocytes to 20 µg/ml, 50 µg/ml, and 100 µg/ml of P25 resulted in 29%, 42%, and 57% loss of urea production, respectively. The exposure of hepatocytes to 20, 50 and 100 µg/ml of anatase resulted in 8%, 20%, and 42% loss of urea production, respectively. The exposure of hepatocytes to rutile resulted in negligible loss of urea production in all three concentrations compared to untreated cells. The comprehensive quantification of urea synthesis for a week demonstrated similar trend when exposed to the different concentrations of the TiO₂ nanoparticles **Fig. 12**.

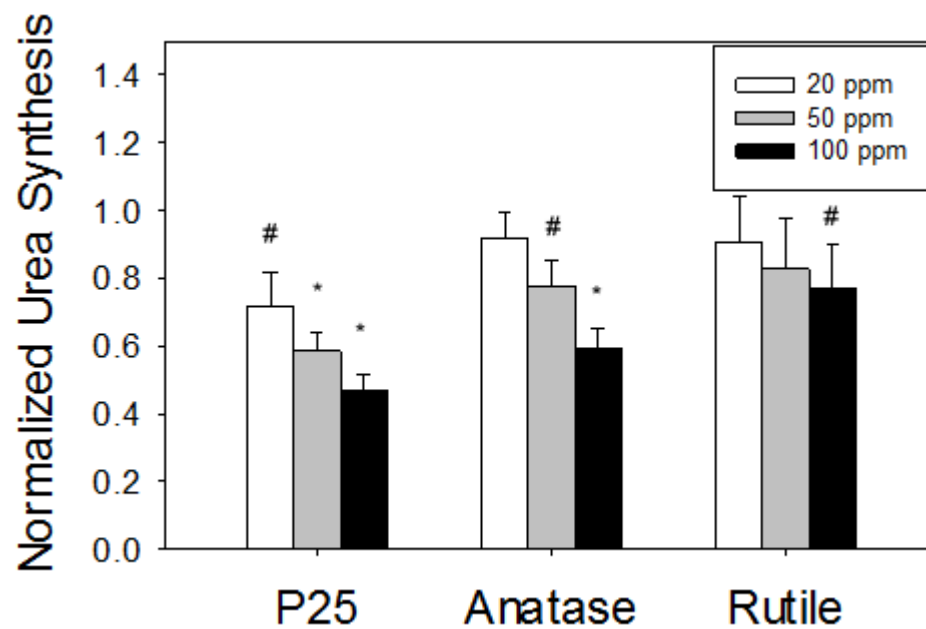


Figure 11. Characterizing the effect of the different TiO₂ nanoparticles treatment on primary hepatocytes specific functions; Quantification of urea synthesized primary hepatocytes after 72 h of exposure normalized to the untreated cells * p value < 0.001,

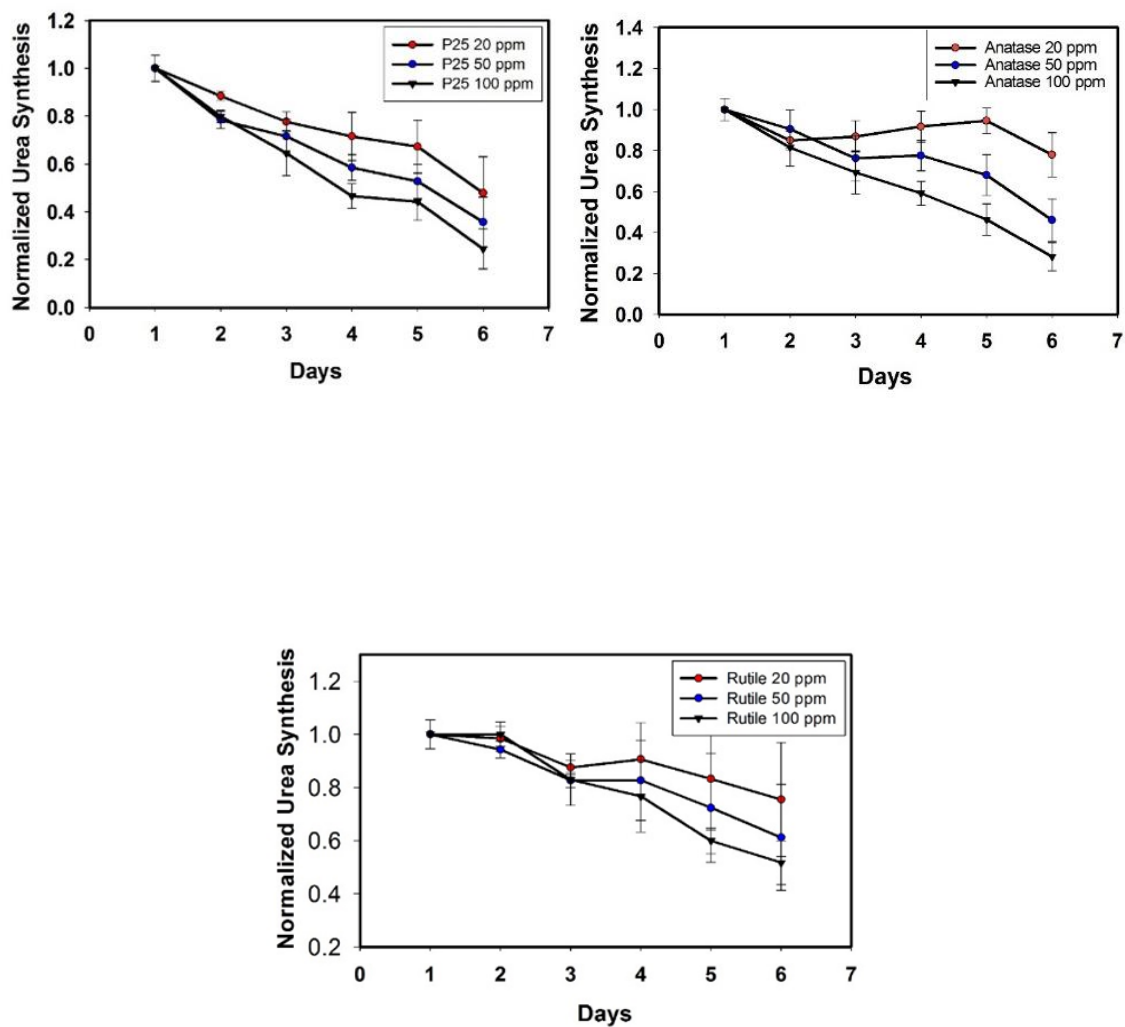


Figure 12. Quantification of urea synthesized primary hepatocytes from day 1 to day 7 in culture when treated with the different TiO₂ nanoparticles. All the data points are normalized to untreated hepatocytes

3.3.3.2 Albumin Synthesis

We further quantified the amount of albumin synthesized using sandwich ELISA technique. **Fig. 13** illustrates the albumin synthesis of primary hepatocytes after 72 h of exposure to different TiO₂ nanoparticles. We observed significant concentration and type dependent loss in albumin synthesis comparable to our data on urea production. The exposure of hepatocytes to 20, 50, and 100 µg/ml of P25 resulted in 27%, 41%, and 60% loss of albumin production, respectively. The exposure of hepatocytes to 20, 50, and 100 µg/ml of anatase resulted in 10%, 20%, and 35% loss of albumin production, respectively. Akin to the urea production, the exposure of hepatocytes to rutile resulted in decreased albumin production in all three concentrations compared to untreated cells. The comprehensive quantification of albumin synthesis for a week demonstrated similar trend when exposed to the different concentrations of the TiO₂ nanoparticles **Fig. 14**.

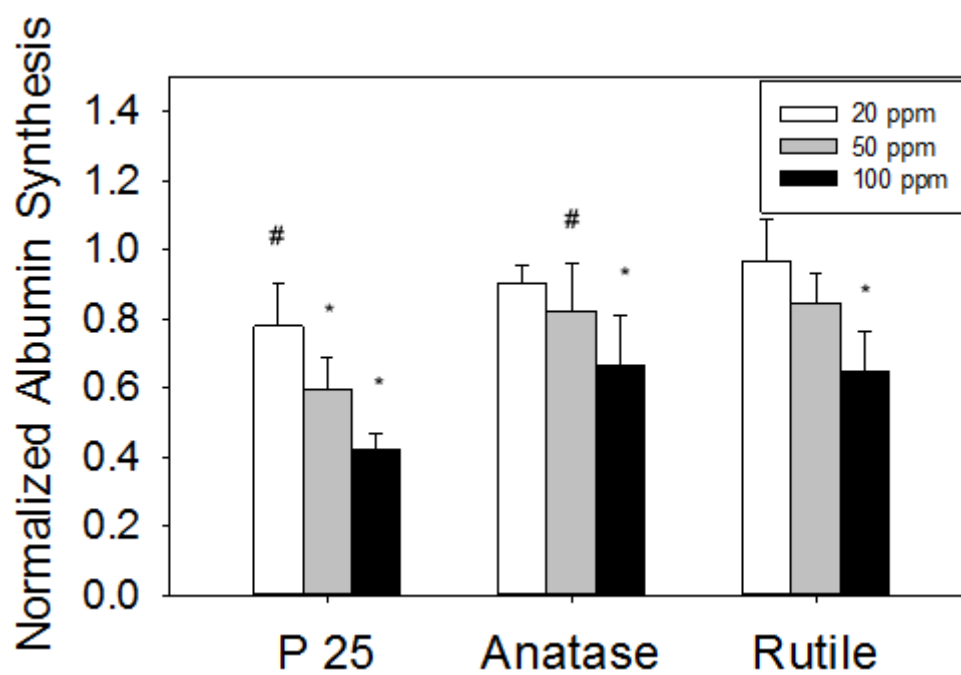


Figure 13. Characterizing the effect of the different TiO₂ nanoparticles treatment on primary hepatocytes specific functions; Quantification of albumin synthesized primary hepatocytes after 72 h of exposure normalized to the untreated cells * p value < 0.001, # p value 0.01

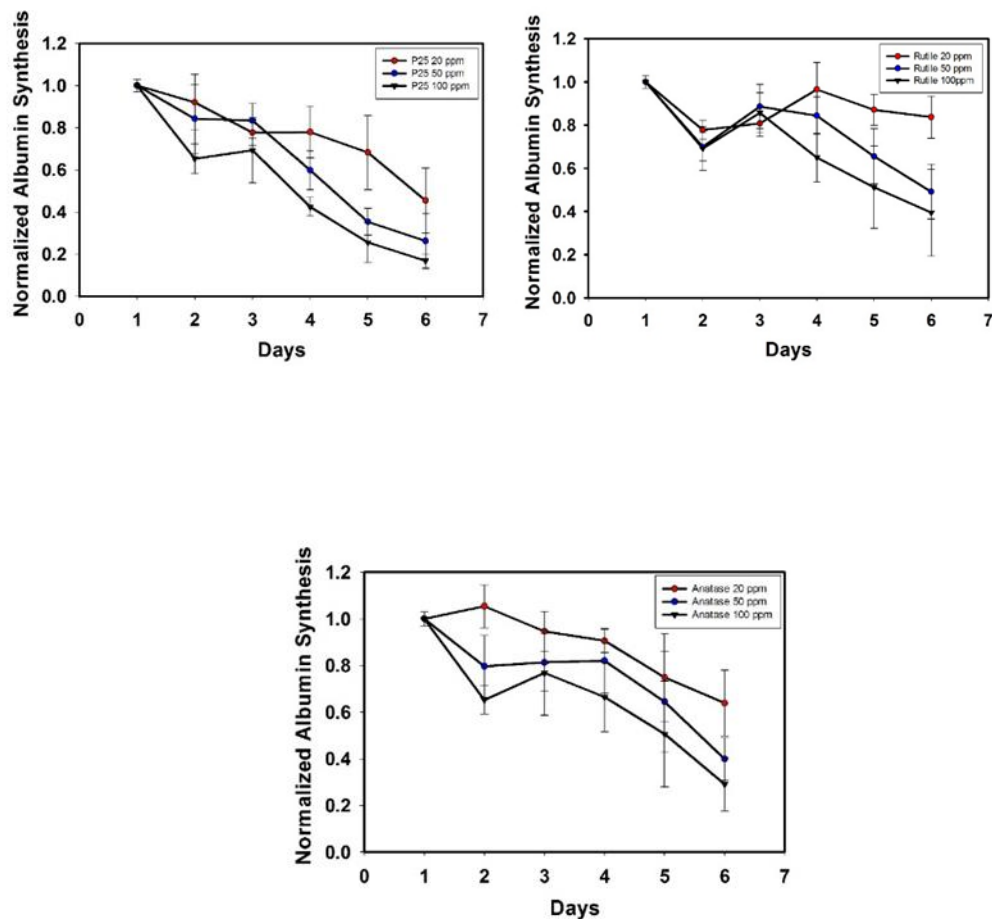


Figure 14. Quantification of albumin synthesized primary hepatocytes from day 1 to day 7 in culture when treated with the different TiO₂ nanoparticles. All the data points are normalized to untreated hepatocytes.

3.4 Discussion

Following the nanoparticle characterization, we studied the cytotoxicity of the different types of nanoparticles using MTT assay (**Table. 2 and Fig. 7**). Our observations are in agreement with some reports^{36, 37} and in disagreement with others³⁸ on the cytotoxicity of TiO₂ nanoparticles. This discrepancy may be due to several reasons including the technique

employed in evaluating cellular changes, such as membrane permeability (live/dead fluorescent staining and trypan blue assays) *versus* mitochondrial function (3-(4,5-dimethylthiazole-2-yl)-2,5-biphenyl tetrazolium bromide or MTT assay)³⁹. Our result indicates that pure anatase and P25 nanoparticles are more cytotoxic compared to rutile nanoparticles. This trend is consistent with previous reports comparing the anatase and rutile TiO₂ nanoparticles.²⁶ This result also provides us with the range of concentration that needs to be addressed to enable complete mechanistic understanding of TiO₂ nanoparticles mediated toxicity in liver cells. These concentrations are in the relevant sub-acute range, as compared to previous studies that have been carried out focusing on effect of TiO₂ nanoparticle exposure on liver^{16, 33, 40, 41} Numerous *in vitro* studies studying the toxicity of TiO₂ nanoparticle have consistently used high concentrations of the nanoparticles, thus limiting these studies to probe mechanistic studies beyond toxicity of the nanoparticles^{26, 42, 43} The purpose of our study is to further investigate how TiO₂ nanoparticles exposure affect primary hepatocytes, with a particular focus on changes in cellular phenotype and mechanisms that mediate these changes. As a result we specifically chose three concentrations of TiO₂ nanoparticles for all the subsequent mechanistic studies (20 µg/ml, 50 µg/ml, 100 µg/ml) with 72 h exposures that is reflective of the LC₅₀ data. These concentrations fall in the sub-lethal range, thereby permitting us to investigate crucial early cellular events, which will yield a better mechanistic understanding of the intrinsic factors mediating nanoparticle induced toxicity.

To determine the effect of the different nanoparticles in the chosen concentration on primary hepatocyte morphology, we used SEM imaging. As seen from **Fig. 8**, the cells did not display a marked change in morphology. Hepatocytes did not exhibit significant change

in aggregate formation or loss in attachment from the culture substrate. Typically cells that are necrotic have distinct surface features in the form of loss of membrane integrity and presence of surface lesions. However, such features were missing in hepatocytes exposed to all three TiO₂ nanoparticles.

Subsequently, we observed compromise in cell viability through MTT assay which was most pronounced in P25 and anatase. The loss in viability was also directly dependent on the concentration of treatment. The loss in viability was not significantly pronounced in rutile treated samples (**Fig. 9**). These results indicate that there is a concentration and type dependent effect on primary hepatocytes when exposed to TiO₂ nanoparticles. Upon extending the treatment time, we also observed drastic loss in cell viability when hepatocytes were exposed to P25 and anatase for one week while exposure to rutile did not show significant change in viability (**Fig. 10**). This difference in the cell behavior reflects on potentially different modes of actions from the different TiO₂ nanoparticles on the hepatic biology.

We examined the effect of TiO₂ nanoparticle treatment on primary hepatocyte specific functions by quantifying urea and albumin synthesis (**Fig.11 to Fig. 14**). Hepatocyte mediated urea production is an indicator of intact nitrogen metabolism and detoxification and albumin synthesis is a widely accepted marker of hepatocyte synthetic function. We observed significant loss in urea and albumin synthesis function of hepatocytes, which was both concentration and type dependent. Exposure to rutile, in line with earlier observations, resulted in the least loss in both urea and albumin synthesis.

Animal studies have shown that damage does occur to the liver when exposed to TiO₂ nanoparticles, however, it is challenging to deduce the effect of nanoparticles on a particular cell type using an *in vivo* study. Limited number of *in vitro* studies has been carried out to understand the direct effect of TiO₂ nanoparticles on liver using primary hepatocytes.^{33, 40, 44, 45} A major weakness of existing literature about the *in vitro* effects of nanoparticles is that the *in vivo* dosimetry and biokinetics are largely ignored, i.e., effects, if observed, are at high concentrations.^{46, 47} There is a deficiency in a conclusive result for the direct effect of these nanoparticles on hepatocytes functions when exposed to lower concentrations of nanoparticles. These results demonstrate that even though the hepatocytes have high viability at 72 h, the exposure to P25 and anatase results in significant damage to hepatic functions. The most critical observation is the exposure to 100 µg/ml of commercially used P25 TiO₂ nanoparticles for 72 h, though has 77% viable cells, results in 60% loss in hepatic functions. We hypothesize that exposure to TiO₂ nanoparticles causes significant stress and damage on important hepatic function even when the cells are viable. This suggests that employing cell viability as a sole marker for effect of environment exposures including nanoparticles is a weak biomarker to identify potential risk factors of these exposures.

3.4 Conclusion

We treated primary rat hepatocytes with different types of TiO₂ Nanoparticles in a range of concentrations to determine the LC₅₀ values that enabled us to select the sub-acute range of 20, 50 and 100 µg/ml as the working concentrations for the cellular studies. Hepatocytes did not exhibit marked changes in cellular phenotype and only a moderate loss in cellular viability at chosen concentrations. We observed a nanoparticle type and concentration dependent loss in urea synthesis and albumin synthesis in primary hepatocytes subjected to treatment and this effect was most pronounced in P25 treatment groups, closely followed by anatase. Rutile treatment resulted in the least loss in hepatocyte functions.

Chapter 4 Mechanistic Aspects of Titanium Dioxide Mediated Toxicity

4.1 Introduction

4.1.1 Titanium Dioxide and Oxidative Stress

Numerous studies have demonstrated that metal oxide nanoparticle induced toxicity is primarily mediated by increased ROS production.^{48, 49} A study on HepG2 cells show ROS mediated DNA damage in the cells, upon treatment with TiO₂ Nanoparticles.⁵⁰ Several studies also demonstrate ROS mediated inflammatory response in the animal models.^{48 23} It is well established that, in excess, ROS species can lead to highly detrimental macromolecular interaction that can further lead to cellular events such as inflammation, mitochondrial damage, membrane disruption and lastly cell death.⁵¹ Mitochondrial function and ROS production are mutually dependent where excessive ROS production leads to mitochondrial stress and stressed mitochondria, in turn, produce more ROS species.⁵² Few studies provide evidence of impaired mitochondrial bioenergetics and apoptotic cell degeneration after low-level exposure to TiO₂.^{23, 24}

4.1.2 The Liver and Mitochondria

Hepatocytes constitute approximately 80% of the liver mass. These cells exhibit high metabolic and bio-transforming activity that consequently imposes high energy requirements. To meet these energy requirements, hepatocytes contain a high density of mitochondria, distributed uniformly throughout the cell body.^{53, 54} Mitochondria act as the vital source of energy in hepatocytes and also play a significant role in extensive oxidative metabolism and normal functioning of the liver.⁵⁵ Inherently, mitochondria have a highly dynamic nature; they undergo continual fission and fusion processes which counterbalance

each other, to alter the organelle morphology that enables the cell to meet its metabolic requirements and cope with internal or external stress.^{56, 57} Three central players that control the process of mitochondrial fission and fusion resulting in the unique structural features, have been identified in mammals: (1) Mitofusins 1 and 2 (Mfn-1 and Mfn-2) ; for outer-membrane fusion (2) OPA1; for inner membrane fusion and (3) Drp1 for inner and outer membrane fission.⁵⁷ In normal conditions, mitochondrial fusion enhances mitochondrial integrity by allowing component sharing across the tubular network. However, fusion of highly damaged mitochondria to the network could be detrimental, since impaired mitochondria generate reactive oxygen species (ROS) that results in significant cellular damage.^{55, 57}

The concern about adverse health effects of low-level exposure to TiO₂ is imperative to address, particularly to analyze whether TiO₂ exposure leading to liver degeneration by impairing mitochondrial bioenergetics. There is a plethora of published literature on acute TiO₂ toxicity, however, the effect of TiO₂ exposure on the hepatocyte mitochondria and its implications on the liver remain to be investigated.

Recent studies demonstrate that several liver diseases, are related to the optimal function of mitochondrial dynamics that leads to differential regulation of the fusion and fission markers discussed above.^{58, 59} Mitochondrial oxidative damage has been demonstrated to be a major factor in several liver disorders such as nonalcoholic steatohepatitis, Wilson's disease, early graft dysfunction after liver transplantation, alcohol induced liver disease, non-alcoholic fatty liver disease, viral hepatitis, cholestasis and chronic hepatitis C.^{53, 60-64} The condition of oxidative stress results in the formation of damaging ROS due to continual

leaking of electrons from the respiratory chain.⁵² Functional impairment of mitochondria, due to oxidative stress, in hepatocytes is often accompanied by modification of mitochondrial proteins, DNA and lipid peroxidation which may lead to mitochondrial bioenergetics failure, that eventually leads to compromise in cellular functions and subsequent necrotic or apoptotic cell death.⁵² Fission protein Drp 1 has been linked to cell death in previous studies.⁶⁵ Diminished OPA1 and Mfn (1 and 2) levels have been reported in biological systems that are in diseased state.⁶⁶ Apart from diseases, recent studies have demonstrated that exposure to several engineered materials, including nanomaterials, leads to structural and functional alterations in mitochondrial membranes.^{67, 68}

In this study we investigated the perturbations in the liver behavior and mitochondrial characteristics caused by exposure to TiO₂ nanoparticles in order to broaden our understanding on the molecular mechanisms of liver dysfunction induced by these highly utilized nanoparticles. We used primary hepatocytes to investigate the concentration and type dependent toxic effects of commercially available rutile, anatase and P25 TiO₂ nanoparticles on mitochondrial dynamics and hepatic functions. The results of our study indicate that TiO₂ nanoparticles induce ROS production, cause mitochondrial damage in hepatocytes and compromise normal liver function.

4.2 Materials and Methods

4.2.1 Reactive Oxygen Species (ROS) Quantification

Reactive Oxygen Species (ROS) production was quantified by a H₂DCFDA based fluorescence assay. Briefly, the cells were washed to remove traces of serum from the culture media and were incubated with 10 μ M H₂DCFDA [Life Technologies, NY] for a

duration of 30 min at 37 °C. After incubation, cells were gently washed and cells were trypsinized using TRYPLE select [Life Technologies, NY] and suspended in PBS. The cell suspension was transferred to a 96 well plate, which was read at excitation 528 nm and emission 405 nm using a SLFA plate reader [Biotek, Winooski, VT]. Hydrogen Peroxide treatment was used as a positive control and the untreated hepatocytes were used as the experimental control to normalize the fluorescence intensity.

4.2.2 Gene Expression Studies

4.2.2.1 RNA and cDNA preparation

At each time point total RNA from primary hepatocytes was isolated using RNeasy Micro Kit [Qiagen, Valenica, CA] according to the manufacturer's instructions. Briefly, cells were trypsinized, centrifuge pelleted, washed with PBS and lysed in RLT buffer with equal volume 70% ethanol. The mix was then centrifuged in an RNeasy spin column, washed and concentrated until the final RNA was released into RNase free water. The quality and quantity was determined by ND-1000 spectrophotometer [NanoDrop Technologies Wilmington, DE] and reverse transcribed using iScript™ cDNA synthesis kit [Bio-Rad Laboratories, CA] by following manufacturer's instructions.

4.2.2.2 qPCR

Quantitative Real Time PCR was performed using SYBR Green Master Mix [Applied Biosystems, Foster City, CA] in an egradient S Mastercycler [Eppendorf, NY]. The primers of interest were obtained from Integrated DNA Technologies [Coralville, IA] with the following sequences: OPA-1 (Forward 5'- CCTGTGAAGTCTGCCAATCC -3' and Reverse 5'- CTGGAAGATGGTGATGGGTT -3'), Mfn1 (Forward 5'-

TCGTGCTGGCAAAGAAGG-3' and Reverse 5'-CGATCAAGTTCCGGGTTC-3'). GAPDH (Forward 5' ATGATTCTACCCACGGCAAG 3' and Reverse 5' CTGGAAGATGGTGATGGGTT 3') was used as the housekeeping gene. The $\Delta\Delta\text{CT}$ method was utilized for analysis of each target gene with respect to the housekeeping gene.

4.2.3 Mitochondrial Morphology Imaging

Mitotracker FM, green stain [Life Technologies, NY] was used for the specific staining of primary hepatocyte mitochondria. Live cells were washed with PBS and the dye was diluted to a concentration of 100 nM in Fluorobrite DMEM [Life Technologies, NY] and added to the cells. Cells were incubated at 37 °C for 45 min and then washed extensively and imaged using confocal microscopy (Olympus FV500 IX 81).

4.2.4 Statistical Analysis

The difference between the various experimental groups was analyzed by a one-way analysis of variance (ANOVA) using the statistical analysis embedded in SigmaPlot Software using Tukey test. Q tests were employed to identify outliers in the data subsets. For statistical analysis of all data, $p < 0.05$ was used as the threshold for significance.

4.3 Results

4.3.1 Titanium Dioxide Nanoparticles and Oxidative Stress

We quantified the ROS production using CM-H₂-DCFDA dye in order to measure the increased oxidized status of the cells in response to nanoparticles exposure (**Fig. 15**). At the concentrations of 20, 50 and 100 µg/ml, a type dependent increase in ROS production was observed when primary hepatocytes were exposed to TiO₂ nanoparticles. The exposure of hepatocytes to 50 µg/ml of P25 and anatase resulted in relatively highest ROS production while exposure of the same concentration of rutile demonstrated lesser ROS production.

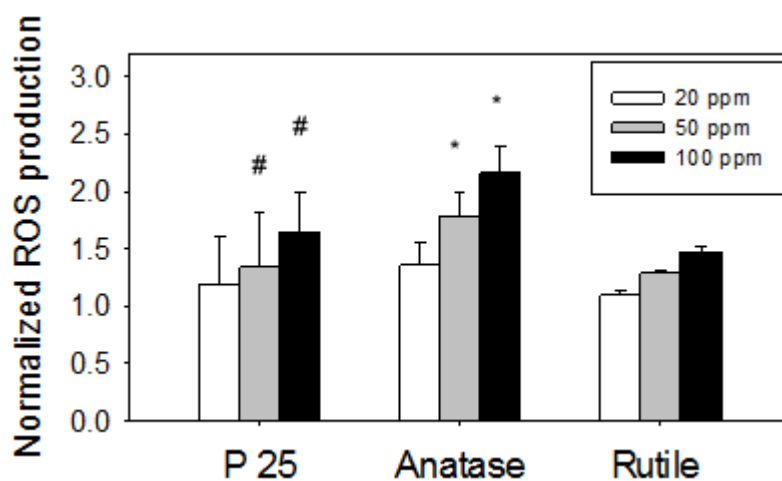


Figure 15. Characterizing the effect of nanoparticle treatment on primary hepatocyte mitochondrial functions; Quantification of Reactive Oxygen Species produced by primary hepatocytes using DCFDA based fluorescence assay after treatment with the different TiO₂ nanoparticles for a duration of 72 h. Significant difference with respect to control is denoted as * p value < 0.0001, # p value < 0.05

4.3.2 Titanium Dioxide Nanoparticles and Mitochondrial Dynamics

To understand the effect of nanoparticle treatment on mitochondrial dynamics, we investigated the relative gene expressions of OPA-1 and Mfn-1 markers associated with mitochondrial fusion events (**Fig. 16**). OPA-1 and Mfn-1 gene expression levels were significantly down-regulated in hepatocytes when exposed to 50 $\mu\text{g/ml}$ P25 and anatase with commercially used P25 having the highest effect. On the contrary, down-regulation of these markers in rutile treatment group was not substantial.

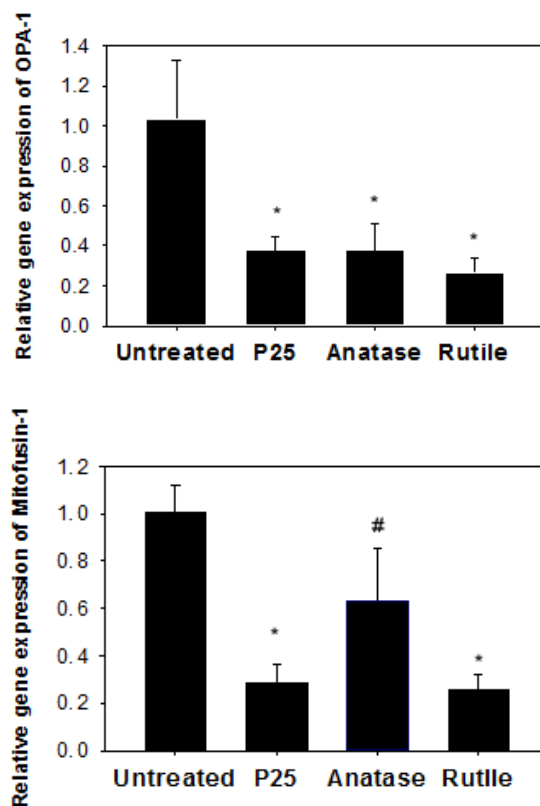


Figure 16. Characterizing the effect of nanoparticle treatment on primary hepatocyte mitochondrial functions; Relative gene expressions of mitochondrial fusion markers when primary hepatocytes are treated with nanoparticles at a concentration of 50 $\mu\text{g/ml}$ as analyzed using qPCR with GAPDH as housekeeping gene. Significant difference with respect to control is denoted as * p value < 0.001 and # p value < 0.05

4.3.2 Titanium Dioxide Nanoparticles and Mitochondrial Morphology

To probe the effect of the nanoparticles on the mitochondrial morphology and integrity, we imaged the mitochondria using the fluorescent stain Mitotracker FM (**Fig. 17**). The untreated primary hepatocytes depicted the typical fiber-like morphology indicating a healthy mitochondria. When hepatocytes were exposed to TiO₂ nanoparticles, there was a significant loss in the fiber-like morphology and presence of high levels of fragmentation was also observed.

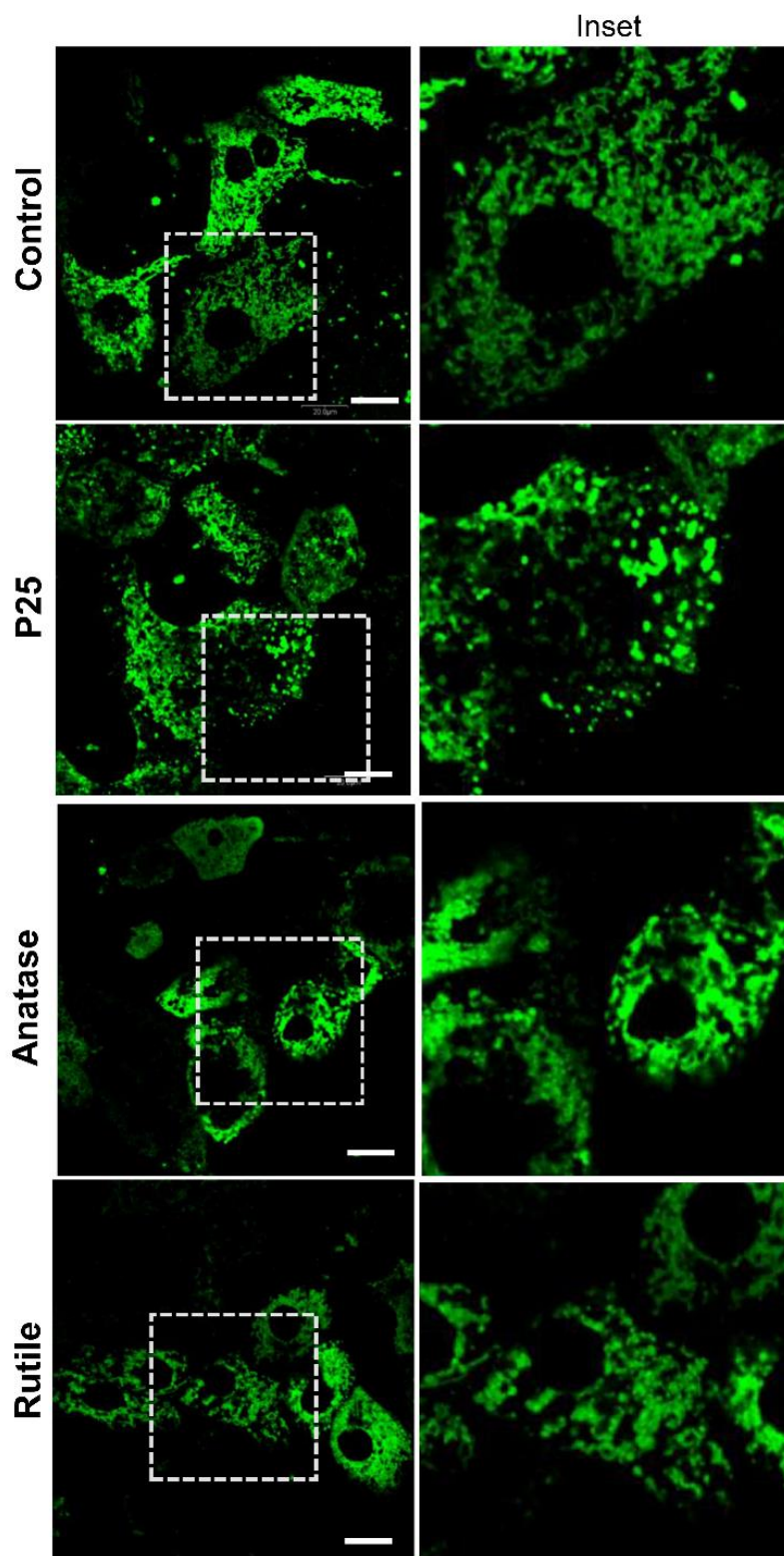


Figure 17. Fluorescent imaging of the mitochondrial morphology in primary rat hepatocytes after treatment with the different TiO₂ nanoparticles at a concentration of 50ppm using Mitotracker green FM. Scale 20 microns.

4.4 Discussion

To determine the underlying mechanism that potentially causes the loss in hepatic functions intracellular levels of ROS, a marker for oxidative stress, was measured in primary hepatocytes exposed to TiO₂ nanoparticles. Numerous studies have demonstrated that metal oxide nanoparticle induced toxicity is primarily mediated by increased ROS production.^{48,49} Our study indicates that anatase and P25 treated samples exhibit increased ROS production (**Fig. 15**). This higher production of ROS in P25 and anatase indicates that primary hepatocytes are in a high stress environment.

In normal physiological conditions, mitochondrion is the main coordinator of ROS production that is key to maintaining a state of redox homeostasis in the cells, thereby protecting it from the damage of oxidative stress.⁵¹ When the ROS production is higher than the normal range, it results in an elevated state of oxidative stress and the cell responds by overworking the anti-oxidative pathways. Increase in ROS levels leads to DNA or protein denaturation, mitochondrial damage, lipid peroxidation, metabolic disorders and ultimately cell apoptosis.⁶⁹⁻⁷³ Several studies demonstrated that various environmental stresses lead to increased ROS production in cells.⁷⁴

Recent studies have emphasized the interrelationship of ROS and mitochondrial health, with respect to metabolic disorders and manifestation of various diseased states.⁷⁵ Excessive ROS causes mitochondrial dysregulation and comprises the mitochondrial dynamics resulting in a cyclic response that leads to excessive production of ROS. Mitochondria are extremely dynamic in nature and undergo continual fission and fusion processes which counterbalance each other, to alter the morphology that enables the cell to

meet its metabolic requirements and cope with internal or external stress. OPA1 and Mfn-1 are markers known to be instrumental in regulating the fusion process in maintaining the mitochondrial dynamics. We observe a significant down-regulation in the gene expression levels of OPA1 and Mfn-1 in the 50 $\mu\text{g/ml}$ treated hepatocytes, whereas, this down-regulation was not observed in rutile samples. (**Fig. 16**) We also investigated the effect of nanoparticle treatment on fission event by probing Drp1, but we do not see a prominent change in the relative gene expression levels (data not shown). This indicates that the normal cellular balance between the fusion and fission events in mitochondria are disrupted by the nanoparticle treatment, through impairment in the fusion process. Mitochondrial fusion is vital in maintaining the respiratory functions of the organelle and any interference in this function can be detrimental to the bio-energetics, thereby causing a cascade of damage in the cells.

Subsequently, we analyzed of the effect of the different nanoparticle treatment on primary hepatocyte mitochondrial morphology, to visualize the effect of disrupted mitochondrial dynamics. **Fig. 17** displays that as compared to healthy untreated hepatocytes, the treated cells have fragmented and swollen mitochondria. Hepatocytes possess a unique mitochondrial organization wherein the mitochondria are spread throughout the cell body unlike other cells where the mitochondria are concentrated around the cell nuclei and concentration decreases radially. Loss in the typical fiber-like morphology and increase in fragmentation is a strong indication of compromise in the mitochondria dynamics. This is also in sync with our observation where OPA-1 and Mfn-1 were significantly down-regulated in hepatocytes exposed to TiO_2 nanoparticles. Defects in mitochondrial fusion result in mitochondria that appear swollen and spherical, instead of fiber-like. Together,

these results provide confirmative proof that exposure to TiO₂ nanoparticles even at concentration as low as 50 µg/ml results in significant mitochondrial damage by interrupting the fusion-fission equilibrium and affecting the mitochondrial dynamics.⁷⁶

4.5 Conclusion

We observe that Titanium Dioxide Nanoparticles lead to a state of Oxidative Stress due to overproduction of Reactive Oxygen Species. ROS production was most upregulated in P25 treated samples, followed by anatase and then rutile. Mitochondrial fusion markers Opa1 and Mfn1 showed a downregulation in the gene expression, indicating towards the disruption of mitochondrial dynamics, through loss in the fusion event. We stained the mitochondrial fibers using Mitotracker and visualized that the nanoparticle treatment of P25 and anatase resulted in abnormal mitochondrial morphology. These results collectively suggest a state of oxidative stress and mitochondrial damage in primary hepatocytes when treated with TiO₂ Nanoparticles.

Chapter 5 Conclusions

Overall, we observed that exposure of primary rat hepatocytes to different types of commercially available TiO₂ nanoparticles cause toxicological effects in the cells. We note a modest loss in cell viability. However, hepatic specific functions, urea and albumin synthesis, are significantly compromised due to TiO₂ nanoparticles exposure within 72 h even at concentrations as low as 20 µg/ml. We observed an increase the amount of intracellular ROS production when hepatocytes are exposed to TiO₂ nanoparticles, which is indicative of oxidative stress related damages. Finally, we observe that exposure to TiO₂ nanoparticles results in significant mitochondrial damage as seen in the down-regulation of OPA1 and Mfn-1, markers that is indicative of the fusion cycle that is key to maintaining the mitochondrial dynamics. This decreased levels of Mfn-1 and OPA1 results in the fragmented mitochondrial network in hepatocytes exposed to TiO₂ nanoparticles and is a strong indicator of the disruption of the mitochondrial dynamics. From these observations, we propose that TiO₂ nanoparticles induce cytotoxicity of hepatocytes by (1) down-regulating the fusion process thus disrupting the mitochondrial dynamics, (2) inducing damages to the mitochondrial morphology, (3) triggering oxidative stress mediated by an increase in ROS production that is associated with loss of cell viability, and (4) inducing loss in hepatic functions including urea and albumin (**Fig. 18**). Therefore, we propose that TiO₂ nanoparticles could potentially contribute to subsequent adverse health effects and the development of liver diseases such as liver fibrosis.

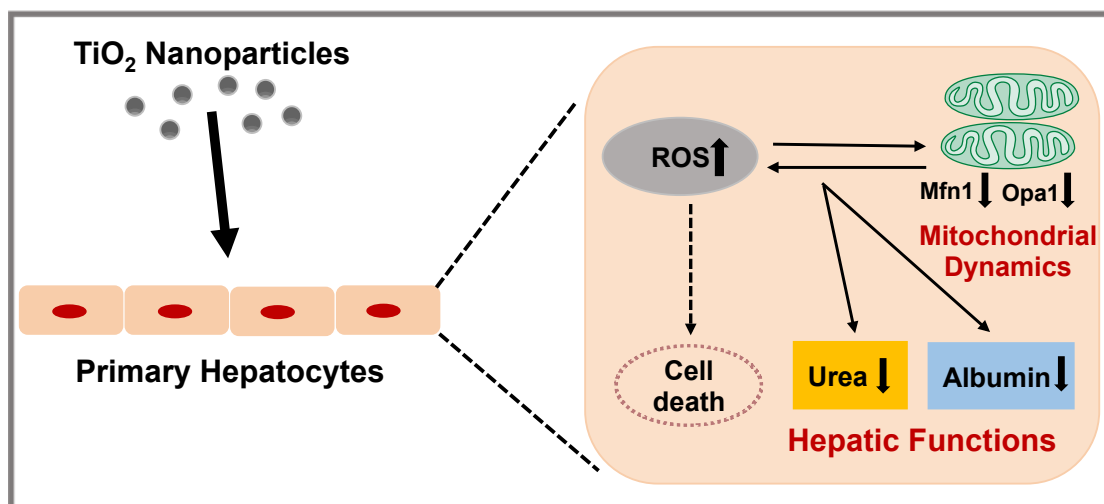


Figure 18. Schematic representation of the possible damaging role of TiO₂ nanoparticles on primary hepatocytes. We propose that TiO₂ induces loss in hepatic functions on primary hepatocytes through the induction of oxidative stress mediated by an increase of ROS production, and significant mitochondria damage by down-regulating the fusion cycle in the mitochondrial dynamics.

Chapter 6 Future Studies

1. Detailed exploration of the biochemical pathways related to mitochondrial respiration and mitochondrial stress mediated cell death pathways will aid in a better understanding of the toxicity effects observed.
2. We also propose that mitochondrial stress has the potential to be used as an early and sensitive marker for nanotoxicological studies and can also supplement studies aimed at designing better therapeutic measures to combat nanomaterial and other engineered materials toxicity.

Bibliography

1. Donaldson, K.; Stone, V.; Tran, C.; Kreyling, W.; Borm, P. J. *Occupational and environmental medicine* **2004**, 61, (9), 727-728.
2. Shi, H.; Magaye, R.; Castranova, V.; Zhao, J. *Part. Fibre Toxicol.* **2013**, 10, (Copyright (C) 2013 American Chemical Society (ACS). All Rights Reserved.), 15.
3. Weir, A.; Westerhoff, P.; Fabricius, L.; Hristovski, K.; von Goetz, N. *Environmental Science & Technology* **2012**, 46, (4), 2242-2250.
4. Anselmann, R. *J. Nanopart. Res.* **2001**, 3, (Copyright (C) 2013 American Chemical Society (ACS). All Rights Reserved.), 329-336.
5. Bahnemann, D. W.; Dillert, R.; Kandiell, T. In *Tailored titanium dioxide nanomaterials: Anatase nanoparticles and brookite nanorods as highly active photocatalysts*, 2010; American Chemical Society: 2010; pp CATL-16.
6. Emerich, D. F.; Thanos, C. G. *Expert Opin. Biol. Ther.* **2003**, 3, (Copyright (C) 2013 American Chemical Society (ACS). All Rights Reserved.), 655-663.
7. Gerhardt, L. C.; Jell, G. M. R.; Boccaccini, A. R. *Journal of Materials Science: Materials in Medicine* **2007**, 18, (7), 1287-1298.
8. Lademann, J.; Weigmann, H. J.; Schafer, H.; Muller, G.; Sterry, W. *Skin Pharmacol. Appl. Skin Physiol.* **2000**, 13, (Copyright (C) 2013 American Chemical Society (ACS). All Rights Reserved.), 258-264.
9. Fujishima, A.; Zhang, X. *C. R. Chim.* **2006**, 9, (Copyright (C) 2013 American Chemical Society (ACS). All Rights Reserved.), 750-760.
10. Lowe, T. *Adv. Mater. Processes* **2002**, 160, (Copyright (C) 2013 American Chemical Society (ACS). All Rights Reserved.), 63-65.

11. Chen, Z.; Meng, H.; Xing, G.; Chen, C.; Zhao, Y.; Jia, G.; Wang, T.; Yuan, H.; Ye, C.; Zhao, F. *Toxicology letters* **2006**, 163, (2), 109-120.
12. Linkov, I.; Satterstrom, F. K.; Corey, L. M. *Nanomedicine: Nanotechnology, Biology and Medicine* **2008**, 4, (2), 167-171.
13. Andersson, P. O.; Lejon, C.; Ekstrand-Hammarström, B.; Akfur, C.; Ahlinder, L.; Bucht, A.; Österlund, L. *Small* **2011**, 7, (4), 514-523.
14. Chen, H.-W.; Su, S.-F.; Chien, C.-T.; Lin, W.-H.; Yu, S.-L.; Chou, C.-C.; Chen, J. J. W.; Yang, P.-C. *FASEB J.* **2006**, 20, (Copyright (C) 2013 American Chemical Society (ACS). All Rights Reserved.), 2393-2395, 10.1096/fj.06-6485fje.
15. Li, N.; Xia, T.; Nel, A. E. *Free Radical Biology and Medicine* **2008**, 44, (9), 1689-1699.
16. Ma, L.; Zhao, J.; Wang, J.; Liu, J.; Duan, Y.; Liu, H.; Li, N.; Yan, J.; Ruan, J.; Wang, H.; Hong, F. *Nanoscale Res. Lett.* **2009**, 4, (Copyright (C) 2013 American Chemical Society (ACS). All Rights Reserved.), 1275-1285.
17. Kim, Y. S.; Kim, J. S.; Cho, H. S.; Rha, D. S.; Kim, J. M.; Park, J. D.; Choi, B. S.; Lim, R.; Chang, H. K.; Chung, Y. H. *Inhalation toxicology* **2008**, 20, (6), 575-583.
18. Echegoyen, Y.; Nerín, C. *Food and Chemical Toxicology* **2013**, 62, 16-22.
19. Blinova, I.; Ivask, A.; Heinlaan, M.; Mortimer, M.; Kahru, A. *Environmental Pollution* **2010**, 158, (1), 41-47.
20. Sharma, V.; Singh, P.; Pandey, A. K.; Dhawan, A. *Mutation Research/Genetic Toxicology and Environmental Mutagenesis* **2012**, 745, (1), 84-91.
21. Meena, R.; Paulraj, R. *Toxicol. Environ. Chem.* **2012**, 94, (Copyright (C) 2013 American Chemical Society (ACS). All Rights Reserved.), 146-163.

22. Yamashita, K.; Yoshioka, Y.; Higashisaka, K.; Mimura, K.; Morishita, Y.; Nozaki, M.; Yoshida, T.; Ogura, T.; Nabeshi, H.; Nagano, K.; Abe, Y.; Kamada, H.; Monobe, Y.; Imazawa, T.; Aoshima, H.; Shishido, K.; Kawai, Y.; Mayumi, T.; Tsunoda, S.-i.; Itoh, N.; Yoshikawa, T.; Yanagihara, I.; Saito, S.; Tsutsumi, Y. *Nat. Nanotechnol.* **2011**, 6, (Copyright (C) 2013 American Chemical Society (ACS). All Rights Reserved.), 321-328.
23. Long, T. C.; Tajuba, J.; Sama, P.; Saleh, N.; Swartz, C.; Parker, J.; Hester, S.; Lowry, G. V.; Veronesi, B. *Environmental Health Perspectives* **2007**, 115, (11), 1631-1637.
24. Park, E. J.; Yi, J.; Chung, K. H.; Ryu, D. Y.; Choi, J.; Park, K. *Toxicology Letters* **2008**, 180, (3), 222-229.
25. Warheit, D. B.; Webb, T. R.; Reed, K. L.; Frerichs, S.; Sayes, C. M. *Toxicology* **2007**, 230, (Copyright (C) 2013 American Chemical Society (ACS). All Rights Reserved.), 90-104.
26. Sayes, C. M.; Wahi, R.; Kurian, P. A.; Liu, Y.; West, J. L.; Ausman, K. D.; Warheit, D. B.; Colvin, V. L. *Toxicol. Sci.* **2006**, 92, (Copyright (C) 2013 American Chemical Society (ACS). All Rights Reserved.), 174-185.
27. Hirakawa, K.; Mori, M.; Yoshida, M.; Oikawa, S.; Kawanishi, S. *Free radical research* **2004**, 38, (5), 439-447.
28. Braydich-Stolle, L. K.; Schaeublin, N. M.; Murdock, R. C.; Jiang, J.; Biswas, P.; Schlager, J. J.; Hussain, S. M. *Journal of Nanoparticle Research* **2009**, 11, (6), 1361-1374.
29. Li, N.; Ma, L.; Wang, J.; Zheng, L.; Liu, J.; Duan, Y.; Liu, H.; Zhao, X.; Wang, S.; Wang, H. *Nanoscale research letters* **2010**, 5, (1), 108-115.

30. Fabian, E.; Landsiedel, R.; Ma-Hock, L.; Wiench, K.; Wohlleben, W.; van Ravenzwaay, B. *Archives of toxicology* **2008**, 82, (3), 151-157.
31. Cui, Y.; Liu, H.; Zhou, M.; Duan, Y.; Li, N.; Gong, X.; Hu, R.; Hong, M.; Hong, F. *Journal of Biomedical Materials Research Part A* **2011**, 96, (1), 221-229.
32. Shi, Y.; Zhang, J.-H.; Jiang, M.; Zhu, L.-H.; Tan, H.-Q.; Lu, B. *Environmental and Molecular Mutagenesis* **2010**, 51, (3), 192-204.
33. Hussain, S.; Hess, K.; Gearhart, J.; Geiss, K.; Schlager, J. *Toxicology in vitro* **2005**, 19, (7), 975-984.
34. Arias, I.; Wolkoff, A.; Boyer, J.; Shafritz, D.; Fausto, N.; Alter, H.; Cohen, D., *The liver: biology and pathobiology*. John Wiley & Sons: 2011.
35. Seglen, P. O. *Experimental Cell Research* **1973**, 82, (2), 391-398.
36. Sha, B.; Gao, W.; Wang, S.; Xu, F.; Lu, T. *Composites Part B: Engineering* **2011**, 42, (8), 2136-2144.
37. Xiong, D.-W.; Fang, T.; Yu, L.-P.; Sima, X.-F.; Zhu, W.-T. *Sci. Total Environ.* **2011**, 409, (Copyright (C) 2013 American Chemical Society (ACS). All Rights Reserved.), 1444-1452.
38. Hu, X.; Cook, S.; Wang, P.; Hwang, H.-m. *Science of The Total Environment* **2009**, 407, (8), 3070-3072.
39. Wang, S.; Yu, H.; Wickliffe, J. K. *Toxicology in Vitro* **2011**, 25, (8), 2147-2151.
40. Linnainmaa, K.; Kivipensas, P.; Vainio, H. *Toxicol. in Vitro* **1997**, 11, (Copyright (C) 2013 American Chemical Society (ACS). All Rights Reserved.), 329-335.

41. Lankoff, A.; Sandberg, W. J.; Wegierek-Ciuk, A.; Lisowska, H.; Refsnes, M.; Sartowska, B.; Schwarze, P. E.; Meczynska-Wielgosz, S.; Wojewodzka, M.; Kruszewski, M. *Toxicology letters* **2012**, 208, (3), 197-213.
42. Chan, J.; Ying, T.; Guang, Y.; Lin, L.; Kai, T.; Fang, Z.; Ting, Y.; Xing, L.; Ji, Y. *Biological trace element research* **2011**, 144, (1-3), 183-196.
43. Reeves, J. F.; Davies, S. J.; Dodd, N. J. F.; Jha, A. N. *Mutation Research/Fundamental and Molecular Mechanisms of Mutagenesis* **2008**, 640, (1-2), 113-122.
44. Shi, Y.; Zhang, J.-H.; Jiang, M.; Zhu, L.-H.; Tan, H.-Q.; Lu, B. *Environ. Mol. Mutagen.* **2010**, 51, (Copyright (C) 2013 American Chemical Society (ACS). All Rights Reserved.), 192-204.
45. Wang, L.; Mao, J.; Zhang, G.-H.; Tu, M.-J. *World J. Gastroenterol.* **2007**, 13, (Copyright (C) 2013 American Chemical Society (ACS). All Rights Reserved.), 4011-4014.
46. Elsaesser, A.; Howard, C. V. *Advanced drug delivery reviews* **2012**, 64, (2), 129-37.
47. Garcia, A.; Espinosa, R.; Delgado, L.; Casals, E.; Gonzalez, E.; Puentes, V.; Barata, C.; Font, X.; Sanchez, A. *Desalination* **2011**, 269, (1-3), 136-141.
48. Liu, S.; Xu, L.; Zhang, T.; Ren, G.; Yang, Z. *Toxicology* **2010**, 267, (1-3), 172-177.
49. Cho, W.-S.; Cho, M.; Jeong, J.; Choi, M.; Cho, H.-Y.; Han, B. S.; Kim, S. H.; Kim, H. O.; Lim, Y. T.; Chung, B. H.; Jeong, J. *Toxicology and Applied Pharmacology* **2009**, 236, (1), 16-24.

50. Shukla, R. K.; Kumar, A.; Gurbani, D.; Pandey, A. K.; Singh, S.; Dhawan, A. *Nanotoxicology* **2013**, 7, (1), 48-60.
51. Droge, W. *Physiological reviews* **2002**, 82, (1), 47-95.
52. Kowaltowski, A. J.; Vercesi, A. E. *Free Radical Biology and Medicine* **1999**, 26, (3-4), 463-471.
53. Hassanein, T. *Mitochondrion* **2004**, 4, (5-6), 609-620.
54. Collins, T. J.; Berridge, M. J.; Lipp, P.; Bootman, M. D. *The EMBO Journal* **2002**, 21, (7), 1616-1627.
55. Treem, W. R.; Sokol, R. J. In *Disorders of the mitochondria*, Seminars in liver disease, 1998; © 1998 by Thieme Medical Publishers, Inc.: 1998; pp 237-253.
56. Frey, T. G.; Mannella, C. A. *Trends in Biochemical Sciences* **2000**, 25, (7), 319-324.
57. Youle, R. J.; Van Der Blik, A. M. *Science* **2012**, 337, (6098), 1062-1065.
58. Olichon, A.; Guillou, E.; Delettre, C.; Landes, T.; Arnauné-Pelloquin, L.; Emorine, L. J.; Mils, V.; Daloyau, M.; Hamel, C.; Amati-Bonneau, P.; Bonneau, D.; Reynier, P.; Lenaers, G.; Belenguer, P. *Biochimica et Biophysica Acta (BBA) - Molecular Cell Research* **2006**, 1763, (5-6), 500-509.
59. Liesa, M.; Palacín, M.; Zorzano, A., *Mitochondrial Dynamics in Mammalian Health and Disease*. 2009; Vol. 89, p 799-845.
60. Arduini, A.; Serviddio, G.; Tormos, A. M.; Monsalve, M.; Sastre, J., Mitochondrial dysfunction in cholestatic liver diseases. In *Front Biosci (Elite Ed)*, 2012; Vol. 4, pp 2233-2252.

61. Bailey, S. M.; Cunningham, C. C. *Free Radical Biology and Medicine* **2002**, 32, (1), 11-16.
62. Lutsenko, S.; Cooper, M. J. *Proceedings of the National Academy of Sciences* **1998**, 95, (11), 6004-6009.
63. Okuda, M.; Li, K.; Beard, M. R.; Showalter, L. A.; Scholle, F.; Lemon, S. M.; Weinman, S. A. *Gastroenterology* **2002**, 122, (2), 366-375.
64. Wei, Y.; Rector, R. S.; Thyfault, J. P.; Ibdah, J. A. *World journal of gastroenterology: WJG* **2008**, 14, (2), 193.
65. Frank, S.; Gaume, B.; Bergmann-Leitner, E. S.; Leitner, W. W.; Robert, E. G.; Catez, F.; Smith, C. L.; Youle, R. J. *Developmental Cell* **2001**, 1, (4), 515-525.
66. Bach, D.; Pich, S.; Soriano, F. X.; Vega, N.; Baumgartner, B.; Oriola, J.; Daugaard, J. R.; Lloberas, J.; Camps, M.; Zierath, J. R.; Rabasa-Lhoret, R.; Wallberg-Henriksson, H.; Laville, M.; Palacín, M.; Vidal, H.; Rivera, F.; Brand, M.; Zorzano, A. *Journal of Biological Chemistry* **2003**, 278, (19), 17190-17197.
67. Alarifi, S.; Ali, D.; Alkahtani, S.; Alhader, M. *Biological trace element research* **2014**, 1-9.
68. Singh, A. V.; Mehta, K. K.; Worley, K.; Dordick, J. S.; Kane, R. S.; Wan, L. Q. *ACS nano* **2014**, 8, (3), 2196-2205.
69. Simon, H. U.; Haj-Yehia, A.; Levi-Schaffer, F. *Apoptosis* **2000**, 5, (5), 415-418.
70. Cabiscol, E.; Tamarit, J.; Ros, J. *International Microbiology* **2010**, 3, (1), 3-8.
71. Yu, B. P. *Physiological reviews* **1994**, 74, (1), 139-162.
72. Kowaltowski, A. J.; Vercesi, A. E. *Free Radical Biology and Medicine* **1999**, 26, (3), 463-471.

73. Loft, S.; Poulsen, H. E. *Journal of molecular medicine* **1996**, 74, (6), 297-312.
74. Valavanidis, A.; Vlahogianni, T.; Dassenakis, M.; Scoullou, M. *Ecotoxicology and environmental safety* **2006**, 64, (2), 178-189.
75. Park, J.; Lee, J.; Choi, C. *PloS one* **2011**, 6, (8), e23211.
76. Chen, H.; Chomyn, A.; Chan, D. C. *Journal of Biological Chemistry* **2005**, 280, (28), 26185-26192.